Redox-linked Proton Transfer by Cytochrome *c* Oxidase

Camilla Ribacka (née Backgren)

Institute of Biotechnology
and
Division of Biochemistry
Department of Biological and Environmental Sciences
Faculty of Biosciences
and
Viikki Graduate School in Biosciences

University of Helsinki

ACADEMIC DISSERTATION

To be presented with the permission of the Faculty of Biosciences of the University of Helsinki for public examination in the auditorium 2402 of Biocenter 3, Viikinkaari 1, Helsinki, on May 4th, at 9 o'clock.

HELSINKI 2007

Supervisor Docent Anne Puustinen
Finnish Institute of Occupational Health
Helsinki, Finland

Reviewers Professor Ilmo Hassinen
Department of Medical Biochemistry and Molecular Biology
Faculty of Medicine
University of Oulu, Finland

Docent Moshe Finel
Drug Discovery and Development Technology Center
Faculty of Pharmacy
University of Helsinki, Finland

Opponent Professor Peter Brzezinski
Department of Biochemistry and Biophysics
Arrhenius Laboratories for Natural Sciences
Stockholm University, Sweden

Kustos Professor Carl G. Gahmberg
Department of Biological and Environmental Sciences
Division of Biochemistry
University of Helsinki, Finland

ISBN 978-952-10-3838-9 (paperback)
ISBN 978-952-10-3839-6 (PDF, http://ethesis.helsinki.fi)

ISSN 1795-7079

Yliopistopaino, Helsinki University Printing House
Helsinki, 2007

To my parents

TABLE OF CONTENTS

LIST OF ORIGINAL PUBLICATIONS

This thesis is based on the following published articles, referred to in the text by their Roman numerals (I-IV):

I **Backgren C**., Hummer G., Wikström M., and Puustinen A. (2000) Proton translocation by cytochrome *c* oxidase can take place without the conserved glutamic acid in subunit I, *Biochemistry 39*, 7863-7867

II Gomes C. M., **Backgren C**., Teixeira M., Puustinen A., Verkhovskaya M. L., Wikström M., and Verkhovsky M. I. (2001) Heme-copper oxidases with modified D- and K-pathways are yet efficient proton pumps, *FEBS Lett. 497*, 159-164

III Wikström M., **Ribacka C**., Molin M., Laakkonen L., Verkhovsky M. and Puustinen A. (2005) Gating of proton and water transfer in the respiratory enzyme cytochrome *c* oxidase, *Proc. Natl. Acad. Sci U.S.A 102*, 10478-10481

IV **Ribacka C**., Verkhovsky M. I., Belevich I., Bloch D. A., Puustinen A. and Wikström M. (2005) An elementary reaction step of the proton pump is revealed by mutation of tryptophan-164 to phenylalanine in cytochrome *c* oxidase from *Paracoccus denitrificans*, *Biochemistry 44*, 16502-16512

ABBREVIATIONS AND SYMBOLS

A	ferrous-oxy intermediate of the binuclear center
ATR FT-IR	attenuated total reflection Fourier transform infrared spectroscopy
CHES	2-(N-cyclohexylamino)ethanesulfonic acid
$\Delta\psi$	electric membrane potential
$\Delta\mu_{H+}$	electrochemical proton gradient across the membrane
DM	*n*-dodecyl-β-D-maltoside
E	the one-electron reduced state of the binuclear center
EPR	electron paramagnetic resonance
eT	electron transfer
F	ferryl-oxy intermediate of the binuclear center
F´	state of the binuclear center after the oxidized enzyme has reacted with H_2O_2
FT-IR	Fourier transform infrared spectroscopy
MES	2-(N-morpholino)ethanesulfonic acid
MV	mixed-valence state of the binuclear center
N-side	negatively charged side of the (inner mitochondrial or bacterial) membrane
O	the fully oxidized form of the binuclear center
$\mathbf{P_M}$	the stable compound formed when MV enzyme reacts with oxygen
$\mathbf{P_R}$	state of the binuclear center after fully reduced enzyme reacts with O_2
P-side	positively charged side of the (inner mitochondrial or bacterial) membrane
R	the unliganded fully reduced state of the enzyme
τ	time constant, 1/*k*
TMPD	*N*,*N*,*N*',*N*'-tetramethyl-1,4-phenylenediamine
Q	ubiquinone
QH_2	ubiquinol
WT	wild-type enzyme

The redox-active metal centers of cytochrome *c* oxidase

Cu_A	the dinuclear copper center in subunit II
Cu_B	the copper center in subunit I
Heme *a*	the low-spin heme in subunit I
Heme a_3	the oxygen-binding, high-spin heme in subunit I
Fe_a	the iron ion of heme *a*
Fe_{a3}	the iron ion of heme a_3

The amino acid numbering is based on the amino acid sequence of *Paracoccus denitrificans*, if not otherwise mentioned.

ABSTRACT

The respiratory chain is found in the inner mitochondrial membrane of higher organisms and in the plasma membrane of many bacteria. It consists of several membrane-spanning enzymes, which conserve the energy that is liberated from the degradation of food molecules as an electrochemical proton gradient across the membrane. The proton gradient can later be utilized by the cell for different energy requiring processes, e.g. ATP production, cellular motion or active transport of ions.

The difference in proton concentration between the two sides of the membrane is a result of the translocation of protons by the enzymes of the respiratory chain, from the negatively charged (N-side) to the positively charged side (P-side) of the lipid bilayer, against the proton concentration gradient. The endergonic proton transfer is driven by the flow of electrons through the enzymes of the respiratory chain, from low redox-potential electron donors to acceptors of higher potential, and ultimately to O_2.

Cytochrome *c* oxidase is the last enzyme in the respiratory chain and catalyzes the reduction of dioxygen to water. The redox reaction is coupled to proton transport across the membrane by a yet unresolved mechanism. Cytochrome *c* oxidase has two proton-conducting pathways through which protons are taken up to the interior part of the enzyme from the N-side of the membrane. The K-pathway transfers merely substrate protons, which are consumed in the process of water formation at the catalytic site. The D-pathway transfers both substrate protons and protons that are pumped to the P-side of the membrane.

This thesis focuses on the role of two conserved amino acids in proton translocation by cytochrome *c* oxidase, glutamate 278 and tryptophan 164. Glu278 is located at the end of the D-pathway and is thought to constitute the branching point for substrate and pumped protons. In this work, it was shown that although Glu278 has an important role in the proton transfer mechanism, its presence is not an obligatory requirement. Alternative structural solutions in the area around Glu278, much like the ones present in some distantly related heme-copper oxidases, could in the absence of Glu278 support the formation of a long hydrogen-bonded water chain through which proton transfer from the D-pathway to the catalytic site is possible. The other studied amino acid, Trp164, is hydrogen bonded to the Δ-propionate of heme a_3 of the catalytic site. Mutation of this amino acid showed that it may be involved in regulation of proton access to a proton acceptor, a pump site, from which the

proton later is expelled to the P-side of the membrane. The ion pair that is formed by the Δ-propionate of heme a_3 and arginine 473 is likely to form a gate-like structure, which regulates proton mobility to the P-side of the membrane. The same gate may also be part of an exit path through which water molecules produced at the catalytically active site are removed towards the external side of the membrane.

Time-resolved optical and electrometrical experiments with the Trp164 to phenylalanine mutant revealed a so far undetected step in the proton pumping mechanism. During the **A** to $\mathbf{P_R}$ transition of the catalytic cycle, a proton is transferred from Glu278 to the pump site, located somewhere in the vicinity of the Δ-propionate of heme a_3. A mechanism for proton pumping by cytochrome *c* oxidase is proposed on the basis of the presented results and the mechanism is discussed in relation to some relevant experimental data. A common proton pumping mechanism for all members of the heme-copper oxidase family is moreover considered.

1. INTRODUCTION

All living organism on Earth require energy in order to stay alive. Plants, algae and cyanobacteria obtain their metabolic energy from photosynthesis, whereas animals acquire their life supporting energy from cellular respiration. Photosynthesizing organisms trap the energy of sunlight using chlorophyll and utilize it for the production of energy-rich carbohydrates from CO_2 and water, with the simultaneous release of oxygen as a by-product. Photosynthetic cyanobacteria were among the first organisms to evolve on Earth, some 3.4 billion years ago. At that time, oxygen was a sparse constituent of the primordial Earth's atmosphere. Photosynthetic reactions eventually increased the atmospheric levels of oxygen. As a consequence, new respiring organisms evolved, which use oxygen as a terminal electron acceptor during their metabolism.

In cellular respiration, different food molecules, such as glucose and fatty acids, are oxidized into CO_2 and water. The released energy is used to synthesize ATP, which serves as a molecular storage of energy. The organism can later extract energy from ATP to drive biosynthesis, motion or active transport of molecules across the membrane. Together photosynthesis and cellular respiration form a steady-state system that is maintained by the energy of the sun.

1.1 The respiratory chain

The respiratory chain (also known as the electron transfer chain) catalyzes the final steps of cellular respiration. It is located in the inner membrane of mitochondria in higher organisms, or in the plasma membrane of archaea and bacteria. The mitochondrial respiratory chain consists of a series of membrane-bound protein complexes and two mobile electron carriers, which transfer electrons from NADH, produced in glycolysis, fatty acid metabolism and the citric acid cycle, to molecular dioxygen (Figure 1). The transport of electrons through the respiratory chain towards electron acceptors of higher potential will release energy. The liberated energy is stored as a proton gradient across the membrane, which can be harnessed for the generation of ATP. The process is known as oxidative phosphorylation.

The first protein complex of the respiratory chain is NADH dehydrogenase, which catalyzes the oxidation of NADH to NAD^+ with the subsequent reduction of ubiquinone (Q) to ubiquinol (QH_2) (reviewed in [1]). This redox reaction is coupled by NADH dehydrogenase to transfer of protons across the membrane by a yet unknown mechanism. The lipid-soluble Q-pool present in the membrane may also receive electrons from membrane bound dehydrogenases, e.g. succinate dehydrogenase (Complex II). Succinate dehydrogenase, a FAD-containing flavoenzyme, oxidizes succinate to fumarate and transfers the electrons to Q (reviewed in [2]). The subsequent enzyme in the respiratory chain, the cytochrome bc_1 complex (Complex III), extracts two electrons from QH_2 in a step-wise manner and transfers them to the water-soluble one-electron carrier cytochrome *c*. The electron transfer reaction is coupled to translocation of two protons across the membrane by the Q-cycle mechanism (see [3] for review).

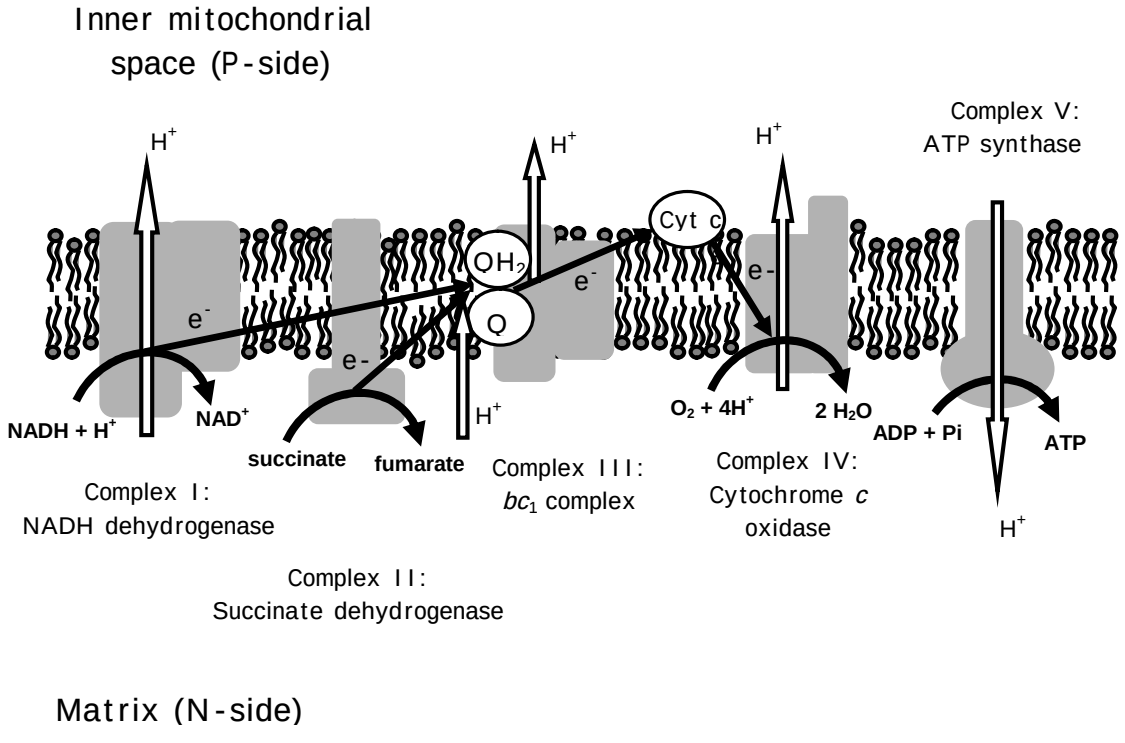

Figure 1. The electron transfer chain and ATP synthase of the inner mitochondrial membrane. Electrons are donated to the chain from NADH or succinate and are thereafter transferred via the Q-pool in the membrane to the bc_1-complex, and from there via cytochrome *c* and cytochrome *c* oxidase to the final electron acceptor, O_2. The flow of electrons through the chain is associated with proton transfer across the membrane, resulting in an electrochemical proton gradient. The flow of protons down their concentration gradient through Complex V: ATP synthase drives the production of ATP from ADP and P_i.

Cytochrome *c* carries electrons to the last enzyme in the respiratory chain, cytochrome *c* oxidase (Complex IV), which reduces the ultimate electron acceptor, dioxygen, to water. The redox reaction is coupled by cytochrome *c* oxidase to translocation of protons across the membrane. The redox-linked proton transfer by complexes I, III and IV of the respiratory chain results in a pH (ΔpH) and charge (Δψ) difference, called the electrochemical proton gradient ($\Delta\mu_{H+}$), between the two sides of the lipid membrane. The $\Delta\mu_{H+}$ is a form of potential energy that can be utilized by different energy-demanding processes in the cell, such as ATP production by ATP synthase, through a controlled flow of protons down their concentration gradient (for review see [4]). The concept of energy conservation through a proton gradient across the membrane was described by Peter Mitchell in 1961 in the chemiosmotic theory [5].

1.2 The family of heme-copper oxidases

Cytochrome *c* oxidase belongs to the vast family of terminal heme-copper oxidases, which reduce molecular dioxygen to water. All heme-copper oxidases contain a low-spin heme and an oxygen-reducing binuclear center, constituted of a high-spin heme and a copper ion. The redox-active metal centers are found in subunit I, where they are ligated by six strictly conserved histidine residues (reviewed in [6]).

The members of the superfamily of heme-copper oxidases can be divided into three main groups (Type A, B and C) based on common structural features in subunit I [7]. Type A oxidases include the mitochondrial cytochrome *c* oxidase and heme-copper oxidases of high similarity. The group is divided further into two subgroups based on the presence (type A1) or absence (type A2) of a conserved glutamate in transmembrane helix VI. Examples of heme-copper oxidases that belong to subgroup A1 are the mitochondrial cytochrome *c* oxidase and the closely related enzymes from bacteria such as *Paracoccus denitrificans* and *Rhodobacter sphaeroides*, as well as the ubiquinol oxidase from *Escherichia coli*. Subgroup A2, which lack the glutamate in helix VI, can be exemplified by the cytochrome *c* oxidases of *caa*$_3$-type from *Rhodothermus marinus* and *Thermus thermophilus*. Heme-copper oxidases that are classified as type B are found in bacteria and archaea. Type B oxidases are a heterogeneous group, which have low sequence homology with the mitochondrial cytochrome *c* oxidase. A characteristic heme-copper oxidase of type B is the *ba*$_3$ oxidase

from *T. thermophilus*. The third group, Type C, differs substantially from both other types of heme-copper oxidases with respect to the amino acid composition. The group consists only of cbb_3 oxidases.

The heme-copper oxidases demonstrate a large flexibility in terms of their electron donors and their heme composition. The prokaryotic oxidases can alternatively contain heme A, B or O or derivatives of heme A and O [8]. In addition, the number of subunits forming the holoenzyme can vary in the prokaryotic oxidases from three to five, whereas the number of subunits in the eukaryotic oxidases is normally higher. Despite large variations in structure, members of all three groups of heme-copper oxidases have been reported to function as proton pumps.

1.3 The terminal oxidases of *Paracoccus denitrificans*

Paracoccus denitrificans is a Gram-negative facultative anaerobic bacterium encountered in soil, sludge and sewage. It belongs to the α subdivision of purple bacteria [9], which are thought to be the precursors of today's mitochondria [10]. The respiratory chain of *P. denitrificans* is very similar to the one found in the mitochondrion [11]. However, on the contrary to the linear respiratory chain of mitochondria (Figure 1), the counterpart in *P. denitrificans* is branched, forming a complex respiratory network [12,13]. The versatility enables *P. denitrificans* to grow on a large variety of different carbon sources aerobically, using oxygen as the terminal electron acceptor or anaerobically, using nitrate, nitrite or nitrogen oxide as the final electron acceptor. Moreover, the flexibility of its respiratory network enables *P. denitrificans* to adapt itself to changes in the oxygen tension of the environment.

P. denitrificans expresses three different oxygen reducing terminal oxidases. One of these is a ba_3-type quinol oxidase [14,15] whereas the other two are cytochrome *c* oxidases. The dominating cytochrome *c* oxidase in *P. denitrificans* is of aa_3-type and is a close structural and functional relative to the mitochondrial cytochrome *c* oxidase [16]. The other cytochrome *c* oxidase is of cbb_3-type, and is expressed only at low oxygen concentrations [17]. All terminal oxidase present in *P. denitrificans* have been shown to pump protons across the plasma membrane [14,18,19].

2. THE STRUCTURE AND FUNCTION OF CYTOCHROME *C* OXIDASE

Cytochrome *c* oxidase is the terminal enzyme in the electron transfer chain of mitochondria and many aerobic bacteria. The enzyme catalyzes the reduction of molecular oxygen to water. At the same time, cytochrome *c* oxidase exploits the energy liberated by dioxygen reduction for translocation of protons across the membrane, against the proton concentration gradient [20]. A total of four protons are pumped per reduced dioxygen molecule, from the matrix or, in case of bacteria, the cytoplasm (the negative or N-side of the membrane) to the intermembrane space or the bacterial periplasm (the positive or P-side of the membrane). The catalytic reaction in itself contributes moreover to the electrochemical proton gradient, since electrons and protons used for water formation are taken up from opposite sides of the membrane. The overall reaction catalyzed by cytochrome *c* oxidase can be described as:

$$4\ \text{Cyt}\ c^{2+}_{\text{(P-side)}} + O_2 + 8\ H^{+}_{\text{(N-side)}} \rightarrow 4\ \text{Cyt}\ c^{3+}_{\text{(P-side)}} + 2\ H_2O + 4\ H^{+}_{\text{(P-side)}}$$

2.1 Overall structure of cytochrome *c* oxidase

The crystal structure of cytochrome *c* oxidase from *P. denitrificans* was unraveled in 1995 [21]. Simultaneously, the x-ray structure of the 13-subunit cytochrome *c* oxidase from bovine heart mitochondria was solved [22]. Although much different in total size, the core part of the two enzymes are structurally much alike. The mammalian oxidase is a large multi-subunit complex with a size of approximately 220 kDa. The core of the enzyme is encoded by the mitochondrial DNA and consists of subunits I-III. The remaining ten subunits are all small globular or transmembrane polypeptides that are encoded by the nucleus. The function of the additional subunits is not completely known, but they may stabilize and protect the catalytically active part of the enzyme [23]. In addition, several binding sites for adenine nucleotides have been found in these subunits, which may imply a regulatory role [24].

Cytochrome *c* oxidase from *P. denitrificans* (Figure 2) consists of four subunits with a total molecular mass of approximately 130 kDa [21]. Three out of the four redox-active metal centers present in cytochrome *c* oxidase are located in subunit I, namely the low-spin heme *a*, the high-spin heme a_3 and the copper ion, Cu_B. Subunit I (Figure 2, in iceblue) is the largest subunit consisting of 12 transmembrane helices. The helices are arranged in groups of four into three semicircles, creating three separate pore-like structures, which extend through the membrane. The low-spin heme, the binuclear center and aromatic residues block the pores, respectively, and prevent free contact between the separate sides of the membrane. All three redox centers of subunit I lie embedded in the intramembrane moiety at a depth of approximately 15 Å from the periplasmic surface and 30 Å from the cytoplasmic surface. The hemes are located in close proximity, where the shortest distance between them is about 4.7 Å [21]. The distance between the heme irons is longer due to the interplanar angle of 108° between heme *a* and heme a_3 [21]. Both hemes are positioned with their propionates facing the P-side of the membrane. Heme *a* is in a low-spin state, where it is ligated by two conserved histidines, His94 from helix II and His413 from helix X. Heme a_3 is in a high-spin state, ligated by His411 from helix X, whereas the sixth coordination position is open. The iron of heme a_3 can, in addition to oxygen, bind various ligands such as carbon monoxide, nitric oxide, cyanide or azide. Heme a_3 is separated from Cu_B by approximately 5 Å, and together they form the active site of oxygen reduction. Cu_B is held in position by three conserved histidine ligands (His276, His325 and His326). The imidazole side chain of one of these, His276, is covalently bonded to the phenol ring of a nearby tyrosine, Tyr280 [25]. The covalent bond between Tyr280 and His276 has a key role in the oxygen splitting mechanism and will be further discussed in chapter 2.6.2.

Subunit I contains in addition two non-redox-active metal centers. A binding site for Mg^{2+} or alternatively Mn^{2+} is located at the interface between subunit I and II, approximately 12 Å above the binuclear center [26-28]. The bound metal is ligated by amino acids from both subunit I and II, as well as three water molecules [26-28]. The Mg^{2+} site is not essential for proton pumping [29], but is likely part of an exit path for water molecules produced at the binuclear center, discussed further in chapter 2.4 [22,30]. The other non-redox-active metal center is found in the external part of subunit I. The binding site is formed by the periplasmic end of helix I and the subsequent loop (loop I-II) together with the loop between helices XI and XII. The site is in *P. denitrificans* and *R. sphaeroides* occupied by a Ca^{2+} ion, while the corresponding site in the mitochondrial cytochrome *c* oxidase houses a Na^+ ion

[26-28]. The physiological role of the bound metal is unclear, but may be related to enzyme stability and regulation [31]. Mutations targeting the Ca^{2+} ligands have revealed that the metal is not necessary for catalytic activity and proton pumping [32,33].

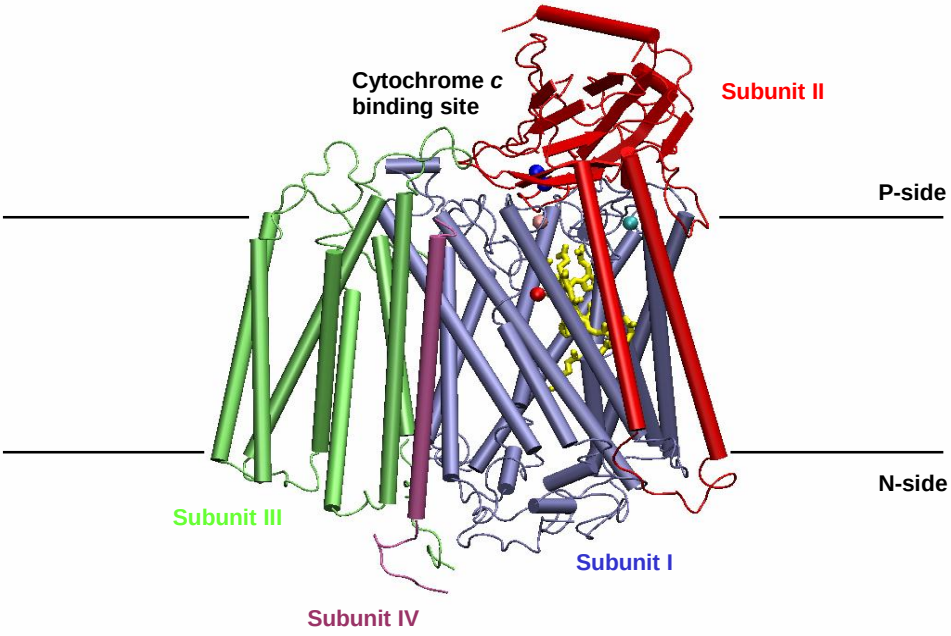

Figure 2. The four-subunit structure of cytochrome *c* oxidase from *P. denitrificans* (Protein Data Bank entry 1QLE, [34]). The subunits are color-coded as follows; subunit I in iceblue, subunit II in red, subunit III in lime and subunit IV in mauve. The redox-active heme groups (yellow) and Cu_B (red sphere) are located approximately 15 Å from the P-side and 30 Å from the N-side of the membrane. The redox-active Cu_A site in subunit II is shown in blue, whereas the non-redox-active Ca^{2+} and Mg^{2+} sites are shown in cyan and pink, respectively. The picture were prepared using the Visual Molecular dynamics software (VMD) [35].

Subunit II (Figure 2, in red) consists of two transmembrane helices and a ten-stranded C-terminal beta barrel, which is located on the P-side of the membrane on top of subunit I. The large periplasmic domain contains one redox-active metal center, a dinuclear copper site called Cu_A, which functions as the primary electron acceptor of cytochrome *c* oxidase. The two copper ions lie at an interatomic distance of ~2.5 Å [26] and are bridged by two cysteins (Cys 216 and Cys 220), and ligated by two histidines (His181 and His 224), one methionine (Met 227) and the carbonyl oxygen of a glutamate (Glu 218). When oxidized, Cu_A is in a mixed-valence [Cu(1.5)-Cu(1.5)] state, and upon reduction the two copper atoms

will equally share the electron [36,37]. The docking site for the electron donor, cytochrome *c*, is located at the interface between subunit II and the external surface of subunit I [38].

Subunit III (Figure 2, in lime) comprises seven transmembrane helices without any redox-active centers. Helix I and II of subunit III are separated from the remaining five helices through a V-shaped cleft, which is occupied by lipid(s) in both cytochrome *c* oxidase from *P. denitrificans* and bovine heart [21,22]. The reason for this structural arrangement is not obvious. It is plausible that the intramembrane lipids facilitate oxygen entry to the binuclear center [39]. Subunit III is not involved in the redox events of cytochrome *c* oxidase, but is important for the stability of the enzyme [40,41]. In the absence of subunit III, increasing amounts of inactive enzyme will appear during catalytic turnover [40,42]. Subunit III may in addition be important for efficient proton uptake via the D-pathway [43,44].

Subunit IV (Figure 2, in mauve) is composed of only one single transmembrane helix. Its function remains a mystery, especially since it bears no significant homology with any other known peptide or protein [21,45]. Deletion of the gene encoding subunit IV has no effect on enzyme expression and activity [45].

2.2 Electron pathways and kinetics of electron transfer

Cytochrome *c* oxidase is reduced by four consecutive one-electron transfer events from cytochrome *c*. The rate-limiting step in the reduction is the formation and dissipation of a complex between the electron donor and acceptor [46]. The interaction between the two is of an electrostatic nature and will strongly depend on the ionic strength of the media [47]. When a stable complex is formed an electron is rapidly transferred from cytochrome *c* to Cu_A of cytochrome *c* oxidase (time constant ~15 µs) [48,49]. The reduction of Cu_A is a pure electron transfer reaction and is not linked to protonation of the enzyme from the aqueous phase [50].

The distance between Cu_A and the iron of heme *a* (Fe_a) is 19.5 Å, whereas the distance between Cu_A and the iron of heme a_3 (Fe_{a3}) is 22.2 Å [26]. In spite of the almost equal distance from Cu_A to heme *a* and heme a_3, electrons are solely transferred from Cu_A to heme *a*, and from thereon to the binuclear center. The rates of electron transfer (eT)

between the redox centers of cytochrome *c* oxidase can be studied by several techniques (see e.g. chapter 4.3). The physiological rate of eT can be studied with photoactivatable one-electron donors that bind to the surface of cytochrome *c* oxidase and promptly release an electron upon the flash of a laser [51]. An electron that is injected this way into the oxidized cytochrome *c* oxidase will reach heme *a*, via Cu_A, within ~10 μs [52]. The flow of electrons in the reverse direction, away from the binuclear center, can be examined by the electron backflow measurement (see chapter 4.3). Two optically distinct phases of eT from the binuclear center to heme *a* and Cu_A appear after dissociation of CO from the mixed-valence enzyme [53,54]. The first phase, which has a time constant of about 3 μs, is accompanied by optical changes at 445 and 605 nm and has thus be ascribed to eT between heme a_3 and heme *a* [54,55]. The second phase, which appears within ~50 μs, has been spectrally assigned to reduction of Cu_A by heme *a* and heme a_3 [54,55].

The three factors that control electron transfer between two different redox-active sites are described by the Marcus theory (reviewed by [56]). These are; 1) the driving force, i.e. the difference in redox potential between the two sites, 2) the distance between them, and 3) the re-organization energy, i.e. the energy needed to alter the structure in response to the change in charge. At the moment, there are at least two different models, which describe how electrons are transferred in proteins. One of these models favor a structural control of the rate of eT, which would accordingly occur through specific electron transfer pathways [57]. The other model postulates that the rate of eT between two redox centers is determined solely by their edge-to-edge distance [58,59]. An extensive study of enzymes, which contain multi-redox centers, supports mainly the latter model [59]. One of the quoted exceptions to the model has been the 3 μs heme a_3→heme *a* eT in cytochrome *c* oxidase, which is approximately 1000 times slower than what would be expected based on the edge-to-edge distance between the hemes [59]. Recently, Pilet *et al*. was able to detect an ultrafast eT between heme a_3 and heme *a* of cytochrome *c* oxidase using femtosecond absorption spectroscopy [60]. The partial eT between the hemes appears within approximately 1.4 ns after CO-photolysis from the mixed-valence cytochrome *c* oxidase [60]. This is close to the calculated eT rate based on the distance between the two hemes and supports the model where eT is purely limited by distance. The major electron transfer event between the hemes takes nevertheless place within the slower 3 μs phase. The complete oxidation of heme a_3 is probably regulated by diffusion of CO out of the enzyme from Cu_B, where it transiently

binds upon dissociation from heme a_3 [60,61]. The rapid nanosecond electron equilibration between the hemes precedes by far the eT that occur during the catalytic cycle (see chapter 2.6), which is limited by internal proton transfer reactions [62].

2.3 Proton input pathways

2.3.1 Proton migration through hydrogen-bonded networks

The conductivity of protons in water is extremely high. The phenomenon originates from the great ability of the water molecule to form hydrogen-bonded networks. In ice, each water molecule is coordinated by hydrogen bonds to four neighboring water molecules, whereas the liquid water molecule participates in three to four hydrogen bonds with its closest neighbors. The structure of bulk water is constantly changing. The fluctuation is due to the reorientation of each water molecule on average every picosecond. As a consequence, the hydrogen bonds between adjacent water molecules are continually broken up and reformed. The result is a rapid proton migration between adjoining water molecules. The mechanistic basis for the proton transfer is explained by a modern version of the Grotthuss mechanism, which was originally described in 1806 [63,64]. A schematic presentation of the mechanism is seen in Figure 3 and it can be briefly described the following way.

An additional proton is at first present at one end of a water chain in the form of a hydronium ion (H_3O^+). Rearrangement of hydrogen bonds moves a proton from this H_3O^+ to an adjacent water molecule, which thus forms a new H_3O^+. Subsequent reshuffling of the hydrogen bonds then transfers another proton from the recently formed H_3O^+ to one of its neighboring water molecule. In this way, protons hop along a hydrogen-bonded chain of water molecules from a proton donor to an acceptor. The proton migration is unidirectional, and a specific proton is not moved *per se*, but due to the reshuffling of hydrogen bonds a proton will ultimately be transferred from one place to another. Before another proton can move in the same direction as the previous one, all water molecules in the chain must reorient themselves to their original position.

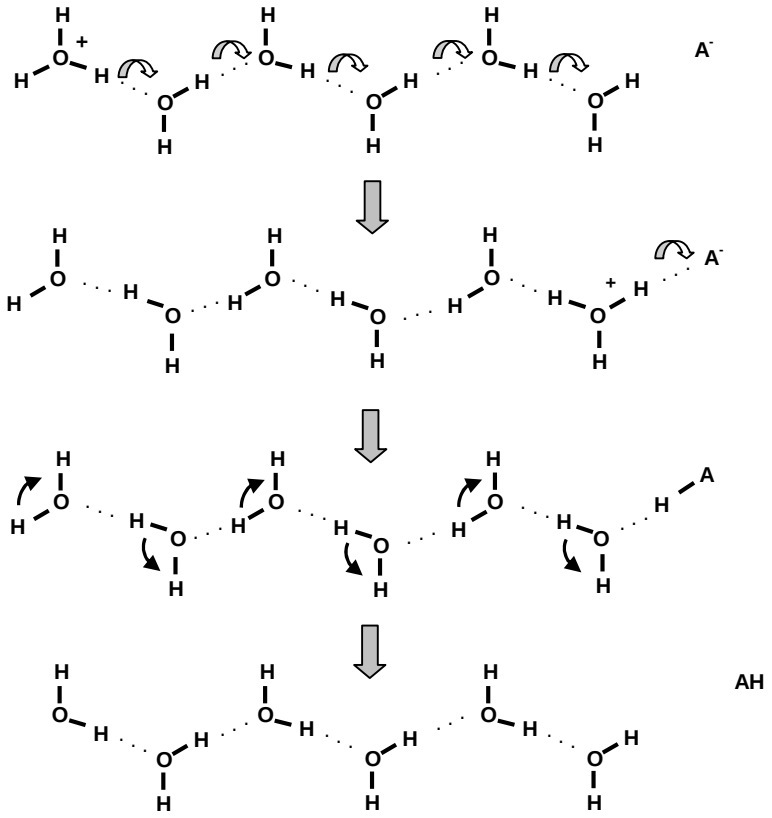

Figure 3. A schematic presentation of proton transfer through a chain of water molecules via a Grotthuss-type of mechanism. An additional proton is present in the form of a H_3O^+ at one end of the water chain. The proton is seemingly transferred from one water molecule to its neighbor, through breakage and formation of new hydrogen bonds, until it finally reaches the proton acceptor (A-) at the other end of the water chain. In order for another proton to be transferred in the same direction the water molecules will have to revert to their original conformation. In the figure, the formation of new hydrogen bonds is marked with white and grey arrows, whereas the reorientation of the water molecules is marked with thin black arrows.

A mechanism similar to the above described Grotthuss mechanism can most likely be applied to intraprotein proton conduction. The hydrophobic nature of the protein interior makes it unsuitable for proton transfer. Instead, protons may be transferred through proton-conducting pathways, which can consist of a single file of hydrogen-bonded water molecules stabilized by protonatable and polar amino acids. This type of proton wire has the potential to transfer protons extremely fast using a Grotthuss-like mechanism [65], especially when the hydrogen-bonded chain is constrained to a narrow hydrophobic space [66].

2.3.2 The K-pathway

The K-pathway is one of the two structurally resolved proton-conducting channels in subunit I of cytochrome *c* oxidase from *P. denitrificans* (Figure 4). It is named after a highly conserved lysine (Lys354), which is essential for the function of cytochrome *c* oxidase [67-69]. The K-pathway leads from the surface of the membrane on the N-side to the vicinity of the binuclear center. Protons enter the channel, presumably, via an invariant glutamate (Glu78) in subunit II and continue via Lys354, a threonine (Thr351) and the hydroxyethylfarnesyl group of heme a_3 up to a tyrosine (Tyr280), located in close contact with the binuclear center. The pathway involves two structurally resolved water molecules. Yet, a hydrogen-bonded network extending all the way from the surface to the active site of cytochrome *c* oxidase is not present without transient structural changes of residues in the channel or movement of internal water molecules [70-72].

The role of Glu78 in the K-pathway is still under debate. Electrostatic calculations have shown that Glu78 alters its protonation state upon reduction of the binuclear center [73]. Mutation of the glutamate in the ubiquinol oxidase from *E. coli* and the cytochrome *c* oxidase from *R. sphaeroides* confirmed a role in proton conduction through the K-pathway [74-76], but the results were contradicted by proton translocation experiments and FT-IR spectroscopy with Glu78 mutants from *P. denitrificans* [77]. Recent electrostatic calculations have confirmed a functional role of Glu78 through its strong electrostatic interactions with Lys354 [78].

The K-pathway is important during the initial reduction of the binuclear center, which precedes binding of dioxygen. Unless accompanied by proton uptake through the K-pathway, electrons will not be transferred to the oxidized binuclear center [79,80]. The K-pathway is not essential for the oxidative part of the catalytic cycle (see chapter 2.6.2) [79,81], but movement of Lys354 may compensate for the additional negative charge at the binuclear center present in the $\mathbf{P_R}$ intermediate [72]. According to recent electrostatic calculations, Lys354 is protonated at neutral pH [78]. Moreover, the pK_a of the residue is raised upon uncompensated reduction of the binuclear center. This implies that the K-pathway is not merely a proton-conducting pathway, but also functions as a “dielectric well”, which can stabilize uncompensated electron transfer to the binuclear center [69].

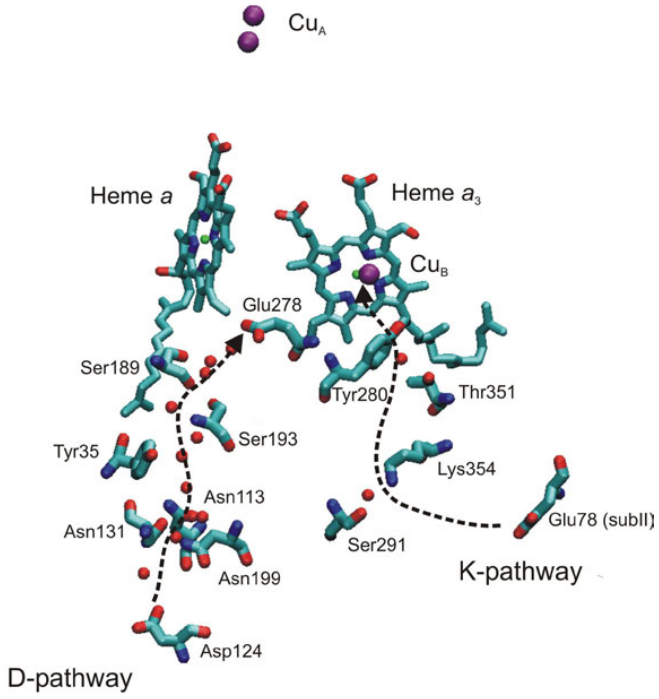

Figure 4. The redox-active centers of cytochrome *c* oxidase together with key residues lining the K- and D-pathways of proton transfer (PDB entry 1M56, [28]). Structurally resolved water molecules in the channels are depicted as red spheres. The picture were prepared using VMD [35].

2.3.3 The D-pathway

The entrance of the D-pathway (Figure 4) is located on the N-side of the membrane in the loop between helices II and III. The loop is rich in charged residues and contains the highly conserved and functionally essential aspartate, Asp124, from which the channel received its name. Mutation of Asp124 to an asparagine abolishes proton translocation and lowers the enzymatic activity dramatically [82-84]. The D-pathway continues from Asp124 via a cluster of conserved asparagines (Asn113, Asn131 and Asn199), a tyrosine (Tyr35) and several serines (Ser 189, Ser192 and Ser193) up to a highly conserved and mechanistically very important glutamate (Glu278). The D-pathway is filled with water molecules, all the way from the protein surface to Glu278 [28], which can facilitate fast proton transfer through a Grotthuss-type of mechanism.

Glu278 is located approximately 10 Å from the active site in a hydrophobic cavity predicted to transiently contain several water molecules [85-87]. The residue is essential for both oxygen reduction and proton translocation [88,89]. The D-pathway is intriguing from a mechanistical point of view, since it conveys two out of the four protons that are consumed

in the formation of water, as well as all four protons that are translocated across the membrane during a single turnover [80,88,90]. Glu278 is believed to be the branching point from where protons are either transferred to the catalytic site (chemical protons) or towards the heme propionates and eventually across the membrane (pumped protons) [21,70,91,92]. Proton transfer via Glu278 is likely to involve movement of its side chain from the downward position in the static crystal structure to an upward position towards the hemes [70,85,92].

2.3.4 The H-pathway

An additional proton-conducting pathway has been proposed based on structural analysis of the mitochondrial cytochrome *c* oxidase from bovine heart [22,27,93]. The so-called H-pathway consists of residues in helices XI and XII of subunit I, and is named after a partially conserved histidine (His448) located close to the channel entrance. The proton route through the H-pathway involves an aspartate (Asp51, bovine numbering), which has no counterpart in the bacterial oxidases. Mutational studies with cytochrome *c* oxidase of bacterial origin do not support a functional role of the H-pathway in the prokaryotic oxidases [94,95].

2.4 Exit paths for protons and water molecules

The area above the heme propionates is rich in structurally resolved water molecules and contains in addition to the previously described Mg^{2+} site (chapter 2.1) two highly conserved arginines, Arg473 and Arg474, which are thought to stabilize the propionates in their deprotonated state [22,26,73]. Mutations of the arginine residues have implicated the Δ-propionate of heme a_3 as the beginning of an exit path for pumped protons [91]. Alternative exit paths for protons that involve the Δ-propionate of heme *a* [96] and propionate A of heme a_3 [97-99] have also been proposed. The hydrophilic region above the hemes is presumably in rapid equilibrium with the P-side of the membrane. Several possible proton exit points may exist at the interface between the membrane and the external part of the enzyme, identified by continuum electrostatic calculations [100]. Of these, the one that

involves Lys171 and Asp173 in subunit II of the mitochondrial cytochrome *c* oxidase is supported by a recent study in which the exposure of backbone hydrogens to the bulk phase in different parts of cytochrome *c* oxidase was investigated by amide H/D exchange detected by mass spectrophotometry [101].

Rapid freeze-quench EPR experiments have revealed that water molecules produced at the binuclear center propagate via the Mg^{2+} site on their way to the P-side of the membrane [30,102]. The exact exit path of the water molecules is not resolved, but it is presumably located at the interface between subunit I and II.

2.5 Oxygen channels

Structural and computational analysis of cytochrome *c* oxidase have identified putative channels through which molecular oxygen can access the active site [22,28,39,70]. For the mitochondrial cytochrome *c* oxidase three different oxygen pathways were proposed based on the structure [22]. One of the channels propagates to the active site via the hydroxyethylfarnesyl group of heme a_3 and another channel approaches via Cu_B. The third proposed oxygen channel of the bovine cytochrome *c* oxidase starts at the V-shaped cleft in subunit III and enters subunit I between helices IV and V at the level of the hemes. This channel coincides with the one suggested based on the structure of cytochrome *c* oxidase from *P. denitrificans* [39]. An alternative starting point for the channel was however proposed for the oxidase from *R. sphaeroides* [28]. The channel is lined by hydrophobic aromatic residues and is hence highly suitable for oxygen diffusion. At its most narrow point, the channel passes between Phe274 and Trp164 [70]. Mutation of a conserved valine (Val279 to Ile mutation) located in this oxygen path dramatically increased the K_M of oxygen compared to wild-type (WT) enzyme, while the V_{max} of the oxygen reaction was essentially the same [39]. In the same V279I mutant, the rate of formation of the oxygen bound intermediate **A** was decreased substantially compared to WT, as well as the subsequent steps of O_2 reduction [103]. The result was interpreted as a partial blockage of oxygen diffusion to the binuclear center by the isoleucine side chain and perturbation of water structure located close to the catalytic site, and supports O_2 delivery to the catalytic site through a specific route.

2.6 The catalytic cycle

The steady-state turnover rate of cytochrome *c* oxidase is very rapid. Cytochrome *c* oxidase consumes on average 300 molecules of oxygen per second and one single turnover of the enzyme is normally completed within five milliseconds. The fully reduced state of the enzyme is unlikely to exist at physiological conditions. Instead, the oxygen reaction is presumably initiated immediately upon oxygen binding to the two-electron reduced enzyme. The full reduction of molecular dioxygen involves four consecutive one-electron transfer steps from the electron donor cytochrome *c* on the P-side of membrane to the active site located in the membrane domain. Each electron addition to the active site is charge compensated by the uptake of a proton from the N-side of the membrane according to the principle of electroneutrality [104,105]. Consequently, one charge is separated across the membrane per electron transferred to oxygen. In addition, the coupled proton pumping by cytochrome *c* oxidase adds to the charge separation, which therefore amount to two charges transferred across the membrane per electron delivered to dioxygen.

The catalytic cycle of cytochrome *c* oxidase is shown in Figure 5. For simplicity, only the redox state of the catalytically active site is shown, which in addition to the binuclear heme a_3-Cu_B center also include Tyr280. The catalytic cycle is usually divided into two parts. The reductive phase (**O→R**), where the active site of cytochrome *c* oxidase receives electrons, and an oxidative phase (**R→O**), where oxygen binds and is reduced to water, with the concomitant oxidation of the enzyme. The cycle involves several intermediate states of the active site, which are commonly denoted by one-letter codes. The intermediate states will be separately described on the following pages.

2.6.1 The reductive phase

The introduction of the catalytic cycle starts with the oxidized and resting state of cytochrome *c* oxidase referred to as **intermediate O**. At this stage, the binuclear center is in a ferric-cupric state and Tyr280 is presumably protonated. The oxidized state of the enzyme exists in different isoforms, which are recognized by their specific absorption spectrum in the Soret region and their diverging EPR signals (reviewed by [106]). The isoforms differ in their rate of reduction as well as their reactivity towards external ligands e.g. cyanide,

hydrogen peroxide and carbon monoxide [107-110]. The as-isolated cytochrome *c* oxidase is sometimes referred to as the slow (or resting) form of the enzyme (**O**) (but see e.g. [111]). The slow isoform can be converted to a fast (or activated) form by full reduction followed by complete oxidation of the enzyme. The formed $\mathbf{O_H}$ intermediate is presumably a metastable state of high energy [112,113]. The energy stored in the $\mathbf{O_H}$ state can be released upon immediate re-reduction of the active site, and will then drive proton pumping across the membrane [112,113]. If the enzyme is not re-reduced within a reasonable time the energy will be lost as the $\mathbf{O_H}$ state decays into the **O** state. The active site in the **O** and $\mathbf{O_H}$ states are thought to differ in their redox properties and bound ligands [112]. Presumably, a water molecule ligates Fe_{a3} in the **O** intermediate, whereas Fe_{a3} in the recently oxidized $\mathbf{O_H}$ intermediate is ligated by a hydroxide anion.

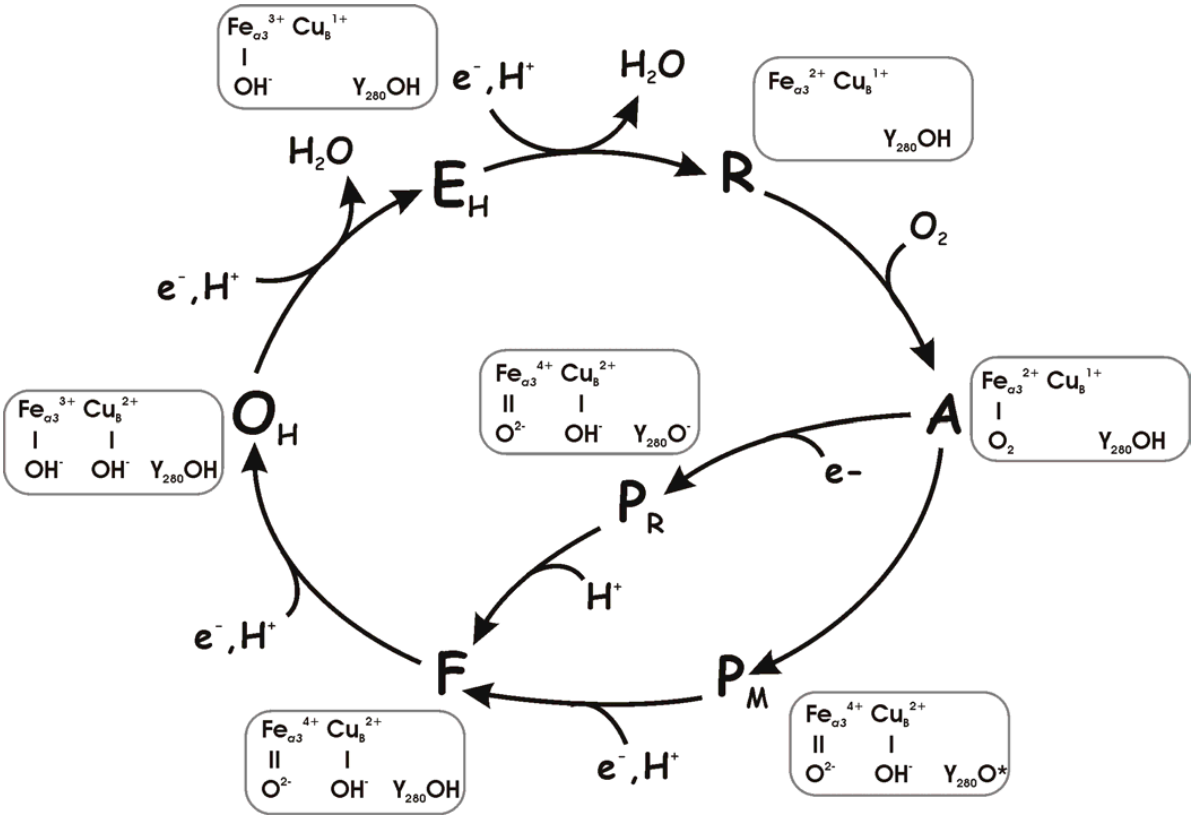

Figure 5. The intermediate states of the catalytic cycle of cytochrome *c* oxidase. The structure of the active site, consisting of heme a_3, Cu_B and Tyr280, at each state of the reaction cycle is shown in boxes. If the two-electron reduced enzyme is allowed to react with O_2, the reaction will follow the outer circle, going from the R→A→P_M→F intermediate. If the fully reduced (four-electron reduced) enzyme is incubated with O_2 the reaction will proceed from the A state via P_R to the F state.

Intermediate E is formed upon arrival of the first electron into the active site. The rate by which an electron arrives from heme *a* is limited by the uptake of a proton from the N-side of the membrane to the active site through the K-pathway [52,62]. The incoming electron reduces Cu_B with simultaneous protonation of its bound hydroxide ion, which is concomitantly released as a water molecule [114]. The transition between the oxidized and one-electron reduced state of the catalytic cycle is associated with proton translocation across the membrane only when the enzyme is reduced shortly after its oxidation (the $\mathbf{O_H \rightarrow E_H}$ transition) [112,113].

Reduction of the active site by a second electron yields the ferrous-cuprous **R intermediate**. The reduction of heme a_3 is accompanied by protonation of the hydroxide ion bound to Fe_{a3}, which is then released as a water molecule. Formation of the **R** intermediate is coupled to proton translocation across the membrane only when the acceptor of the second electron is the $\mathbf{E_H}$ state of the binuclear center, formed from the recently oxidized $\mathbf{O_H}$ state [113,115].

2.6.2 The oxidative phase

The oxidative phase of the catalytic cycle is initiated by the binding of dioxygen to the reduced binuclear center. The formed ferrous-oxy adduct of the active site is called **intermediate A**. In an O_2 saturated environment (~1.2 mM O_2), intermediate **A** is detected by a characteristic absorption peak at 595 nm that appears within ~10 μs after mixing with the fully reduced cytochrome *c* oxidase [116,117].

In the subsequent reaction step, the O-O bond of the bound dioxygen molecule is broken and two incompletely protonated water molecules are formed in a concurrent four-electron reduction step. The produced state of the binuclear center is called the **P intermediate**. The name originates from the previous notion that heme a_3 in this intermediate was in a peroxy state (Fe_{a3}^{3+}-O=O^{2-}) with an intact dioxygen bond [118,119]. However, it is now well established by various experimental studies that the active site in the **P** intermediate is an oxo-ferryl state (Fe_{a3}^{4+}=O^{2-}) with an hydroxide ion bound to Cu_B^{2+} [120-123]. Since formation of the **P** intermediate is not associated with proton uptake from the bulk solution the proton required for hydroxide formation must be extracted within cytochrome *c* oxidase [124-127]. Two out of the four electrons that are needed for the scission of the dioxygen bond are derived from heme a_3 by its oxidation from ferrous to

ferryl state (heme $a_3^{2+} \rightarrow$ heme a_3^{4+}). One is derived from Cu_B by its oxidation from cuprous to cupric state ($Cu_B^{1+} \rightarrow Cu_B^{2+}$). The origin of the fourth electron can be either heme *a* or Tyr280 depending on the initial redox state of the enzyme (see below).

A mixed-valence state of cytochrome *c* oxidase, where the binuclear center is reduced and heme *a* and Cu_A are oxidized, is produced by incubation of the oxidized enzyme with carbon monoxide. Laser flash mediated dissociation of the CO bound to the reduced binuclear center allows O_2 to bind, whereafter an intermediate state called $\mathbf{P_M}$ spontaneous appears (time constant ~150 μs) [128,129]. The fourth electron required for the splitting of the dioxygen bond upon formation of $\mathbf{P_M}$, as well as the proton needed for hydroxide formation at Cu_B, are presumably extracted from Tyr280, which turns into a neutral tyrosyl radical [130-132]. The radical formation is favored by the unusual crosslink between Tyr280 and His276, one of the ligands of Cu_B [25-27].

If the fully reduced cytochrome *c* oxidase is allowed to react with O_2 formation of intermediate **A** is followed by a fast (time constant ~20 μs) transition in which an electron is transferred from heme *a* to the binuclear center with the simultaneous scission of the dioxygen bond [129]. The formed state of the binuclear center is called $\mathbf{P_R}$, where R refers to the fully reduced nature of the enzyme at the start of the reaction [128]. The proton consumed upon formation of the Cu_B-bound hydroxide ion is presumably extracted from Tyr280.

The $\mathbf{P_R}$ and $\mathbf{P_M}$ intermediates have the same absorption spectra, which is characterized by an absorption peak at 607 nm in the alpha region [128,133]. Yet, the $\mathbf{P_M}$ intermediate has, in comparison to the $\mathbf{P_R}$ intermediate, one less electron at its catalytically active site. The $\mathbf{P_M}$ intermediate is long-lived and will exist until cytochrome *c* oxidase receives additional electrons [129]. The $\mathbf{P_R}$ intermediate is on the contrary unstable and will quickly decay into the subsequent **F** intermediate without additional electron transfer to the binuclear center.

Intermediate F appears (time constant ~50 μs) upon protonation of the $\mathbf{P_R}$ state by a proton arriving from Glu278 in the end of the D-pathway [88]. The proton acceptor at the active site is most likely the tyrosinate ($Y280^-$) formed in the preceding step of the catalytic cycle [132,134]. Proton transfer to the active site is accompanied by the partial transfer of the last electron from Cu_A to heme *a* [135] and reprotonation of Glu278 via the D-pathway [136].

The appearance of intermediate **F** can be detected optically by a broad, absorption peak at 580 nm in the alpha region [118]. The transition from the $\mathbf{P_R}$ state to **F** is associated with pumping of one proton across the membrane [137,138].

The $\mathbf{P_M}$ intermediate, formed from the mixed-valance enzyme, will turn into the **F** state when cytochrome *c* oxidase receives an additional electron that is transferred into the active site. The electron will presumably reduce the neutral tyrosyl radical present in the $\mathbf{P_M}$ state, which is simultaneously protonated from the D-pathway via Glu278 [129,139]. The transition from $\mathbf{P_M}$ to **F** is accompanied by translocation of a proton across the membrane.

The final step in the catalytic cycle, $\mathbf{F \rightarrow O_H}$ transition (time constant ~1.5 ms), occurs with the transfer of the fourth electron into the active site and the simultaneous uptake of a proton via the D-pathway [81,140]. This transition is coupled to proton pumping across the membrane [137,138].

2.7 Proton transfer across the membrane

2.7.1 Requirements of a redox-linked proton pump

There are two ways to couple exergonic electron transfer to active proton translocation across a lipid membrane. One way is by a redox loop mechanism, where the redox center that is reduced by an electron simultaneously accepts a proton. The proton is then co-transported with the electron across the membrane, and is released on the other side upon the oxidation of the redox center. The other way is by a proton pump mechanism, where the redox center that accepts an electron not necessarily also accepts a proton. The minimum requirement of a redox-linked proton pump is, in addition to a redox center, a protonatable group that can bind a proton from one side (input side) and release to the other side of the membrane (output side). The protonatable group, hereafter referred to as the pump site, has to control or *gate* proton access to the different sides of the membrane, since uncontrolled diffusion of protons would short-circuit the electrochemical proton gradient [105,141,142].

Proton translocation by a proton pump can be divided into four elementary steps; 1) uptake of a proton to the pump site from the N-side of the membrane, 2) establishment of a protonic connection between the pump site and the P-side of the membrane, 3) release of the proton to the P-side of the membrane, and 4) re-establishment of a protonic connection

between the pump site and the N-side of the membrane. The uptake and release of protons by the pump site can be regulated by changes in its proton affinity (pK_a) or in its conformation. In a redox-linked proton pump, the proton translocation across the membrane is linked to the redox reaction at the redox center. The coupling can be thermodynamic, where protonation of the pump site is coupled to the reduction of the redox center [143,144]. This means that the pK_a of the pump site is modulated by the redox state of the redox center, and reciprocally, the midpoint potential of the redox center is modulated by the protonation state of the pump site. The other alternative is a kinetic coupling, where the pK_a of the pump site is not necessarily regulated by the redox state of the redox center. A state where the redox center is reduced and the pump site is protonated may in this scenario be present in only a fraction of the enzyme population. The transition from the proton input to the output state may still be kinetically favored by a rapid rate constant [145].

2.7.2 Mechanisms for proton translocation by cytochrome *c* oxidase

The exact mechanism by which cytochrome *c* oxidase couples O_2 reduction to translocation of protons across the membrane remains ambiguous despite almost 30 years of extensive studies. During the years, several different coupling mechanisms have been proposed and later discarded. Only a few of the recent theories will be mentioned below.

Throughout the 1990s, cytochrome *c* oxidase was believed to pump protons only during the oxidative part of the catalytic cycle [146]. The assumption was based on the fact that only the **P→F** and **F→O** transitions are associated with a large enough energy release to drive protons across the membrane [147]. The **P→F** and **F→O** steps were believed to pump two protons each based on the equal amount of charge moved relative to the membrane in each transition in electrometrical measurements [148]. In 1999, Michel questioned this idea and suggested that one proton is pumped during the reductive phase of the catalytic cycle [149]. Concomitantly, Verkhovsky and co-workers showed by time-resolved measurements of membrane potential ($\Delta\Psi$) generation that protons are translocated both in the reductive and oxidative phase of the catalytic cycle [112]. The reductive phase is however only coupled to proton pumping if it occurs directly upon enzyme oxidation. A high-energy oxidized state of the binuclear center, called **O~** and later $\mathbf{O_H}$, was proposed that would preserve the energy

from O_2 reduction in the oxidative phase to be used for proton pumping in the subsequent reductive phase [112].

The proton pumping steps of cytochrome *c* oxidase is outlined in Figure 6. Each electron addition from cytochrome *c*, via heme *a* to the binuclear center is accompanied by the uptake of one substrate proton to the active site and the translocation of another proton across the membrane (the $\mathbf{O_H \rightarrow E_H}$, $\mathbf{E_H \rightarrow R}$, $\mathbf{P_{M/R} \rightarrow F}$ and **F→O** transitions) [112,113,115]. The mechanism of vectorial proton transfer is presumably the same in each proton-pumping step, and will consequently be repeated four times during each enzymatic turnover. Proton pumping coupled to the $\mathbf{P_R \rightarrow F}$ transition has gained particular interest when possible mechanisms for proton translocation are discussed, since formation of the **F** state is not linked to electron transfer to the binuclear center, which occurs already in the preceding $\mathbf{A \rightarrow P_R}$ transition.

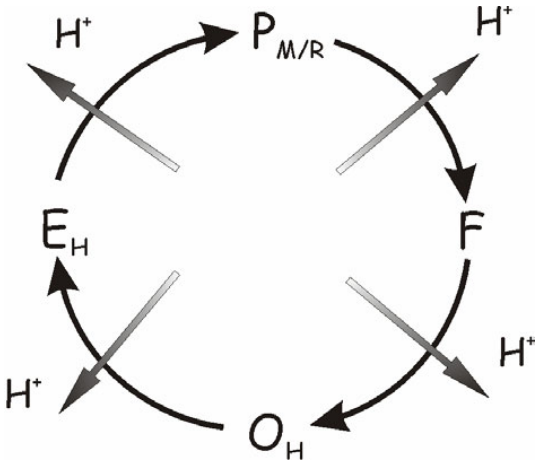

Figure 6. The proton pumping steps in the catalytic cycle of cytochrome *c* oxidase during continuous enzymatic turnover. The $\mathbf{O_H \rightarrow E_H}$, $\mathbf{E_H \rightarrow R}$, $\mathbf{P_{M/R} \rightarrow F}$ and **F→O** transitions are each coupled to translocation of one proton across the membrane.

All recently proposed proton-pumping mechanisms are in compliance with the principle of electroneutrality, according to which introduction of an electron into the low dielectric membrane environment is energetically costly, and must be charge compensated by the uptake of a proton [105]. Michel and Papa *et al*. suggest mechanisms where electron arrival to heme *a* is coupled to uptake of a proton to the pump site [149,150]. Yoshikawa *et al.*

propose a mechanism where the pump site is protonated upon oxidation of heme *a* [93]. Several groups argue that proton pumping is coupled to reduction of the binuclear center instead of heme *a*. Based on electrostatic calculations, Stuchebrukhov and co-workers introduce a proton pumping mechanism that involves redox-state dependent protonation/deprotonation of one of the histidine ligands of Cu_B [97]. Brzezinski *et al*. have proposed a model for proton pumping that originates from structural differences between the WT and the Glu278Gln mutant of *R. sphaeroides* [138,142]. In their view, deprotonation of Glu278 upon proton transfer to the binuclear center leads to structural changes around Glu278, which will propagate through the protein and alter the pK_a and proton accessibility of an accepting group located close to the heme propionates. According to their model, the substrate proton will move to the binuclear center prior to protonation of the pump site. Wikström and colleagues have presented a mechanism whereby proton translocation is gated by the distinct behavior of water molecules in hydrophobic cavities [151]. In their model, the orientation of the water molecules in the cavity next to the binuclear center are affected by the redox-state dependent electric field between heme *a* and heme a_3/Cu_B. When heme *a* is reduced, the pump site, which is located somewhere in the vicinity of the Δ-propionate of heme a_3, will be protonated from Glu278 via a chain of hydrogen-bonded water molecules. Upon electron transfer to the binuclear center, the waters in the cavity will change their orientation, allowing a substrate proton to enter the catalytic site. The protonation of the binuclear center will subsequently expel the proton at the pump site out of the enzyme [151]. It has been argued that this model cannot explain proton pumping in the $\mathbf{P_R \rightarrow F}$ transition, which merely involves protonation of the active site.

3. AIMS OF THE STUDY

The D-pathway of cytochrome *c* oxidase conducts all pumped protons and two out of the four chemical protons that are consumed at the catalytically active site, from the bulk on the N-side of the membrane to the vicinity of the binuclear center. In many enzymes of the heme-copper oxidase family, the D-pathway ends at a highly conserved glutamate (Glu278) that is essential for the oxygen reaction and the uptake and translocation of protons. However, not all members of the heme-copper oxidase family have a glutamate at this location. There are examples of heme-copper oxidase that lack a corresponding glutamate and nevertheless function as true proton pumps.

One of the goals of this thesis was to investigate the role of Glu278 in proton conduction and to explore the possible differences in proton translocation mechanisms between different subgroups of heme-copper oxidases.

The other main focus of this thesis has been to study the beginning of a possible exit pathway for pumped protons and water molecules produced at the binuclear center. Molecular dynamics simulations have shown that redox-changes of the hemes determine the directionality of a hydrogen-bonded water chain, which is located in the cavity between heme *a* and the binuclear center. The chain of water molecules will alternatively conduct protons from Glu278 to the binuclear center or to the Δ-propionate of heme a_3. In the latter configuration, the chain of water molecules is supported by the invariant Trp164, which is hydrogen bonded to the Δ-propionate of heme a_3.

The role of Trp164 in proton translocation was studied both experimentally and theoretically by mutating it to a phenylalanine. In addition, the properties of the salt bridge between the Δ-propionate of heme a_3 and the highly-conserved Arg473 were studied by molecular dynamics simulations.

4. METHODOLOGY

4.1 Isolation of cytochrome *c* oxidase

The *ctaDII* gene encoding subunit I of cytochrome *c* oxidase from *P. denitrificans* has previously been isolated and cloned into a derivative of the broad-host strain expression plasmid pBBR1MSC [94,152,153]. The expression plasmid was transformed into the *E. coli* strain SM10, which was then conjugated with the *P. denitrificans* strain AO1, from which the chromosomal copies of the *ctaDII* gene and its isogene *ctaDI* were deleted, but where the genes encoding the additional subunits of cytochrome *c* oxidase are still present [94]. In the present study, a six-histidine long tail was attached in the end of the *ctaDII* gene to facilitate enzyme purification through affinity chromatography. Mutants of cytochrome *c* oxidase were made by the previously described site-directed mutagenesis protocol [32] and verified by DNA-sequencing (ABI PRISM 310 Genetic Analyzer, Applied Biosystems) during all individual steps of the production. In addition, the DNA sequence of cell samples of fermentor cultivations and smaller cultivations used for proton pumping measurements in whole cells where always examined. Bacterial growth conditions and isolation of cytochrome *c* oxidase from bacterial membranes was performed as earlier described [32], with the exception of the additional Ni^{2+}-NTA affinity chromatography (**paper IV**). The steady-state oxygen reducing activity of the isolated cytochrome *c* oxidase was determined polarographically using a Clark-type oxygen electrode. The electron donor, cytochrome *c* was kept in its reduced state by ascorbate plus TMPD. A more specified description of the experimental conditions is found in **Paper I** and **Paper IV**. The activities of the different mutants were compared to that of WT enzyme.

4.2 Multi-turnover proton pumping measurements

Multi-turnover proton pumping was measured with isolated cytochrome *c* oxidase incorporated into proteoliposomes, or with whole cell preparations (sphaeroplasts), using the oxidant pulse method described below [154,155]. Reconstitution of the isolated enzyme into proteoliposomes was achieved by slow removal of detergent from an enzyme-

detergent-lipid mixture using increasing amounts of BioBeads (Bio-Rad Laboratories) [137,156]. The procedure for incorporation of cytochrome *c* oxidase into vesicles was the same for proton pumping experiments and for electrometry (see below). The enzyme concentration in the initial mixture was 0.5 μM in the reconstitution for pumping experiments and 6.5 μM in the reconstitution for electrometry. The proton permeability of the formed proteoliposomes was determined by the respiratory control ratio (RCR), i.e. the ratio between enzyme activity in the presence and absence of $\Delta\mu_{H+}$, and was typically 3-9 for vesicles used in proton pumping experiments and 2-5 for vesicles used in electrometry. The sphaeroplasts used for proton translocation measurements were prepared by lysozyme treatment and kept in a hypertonic medium [14]. In the proton pumping measurement, proteoliposomes (or sphaeroplasts) were kept in an anaerobic container under constant argon flow in the presence of excess reductant plus valinomycin, which dissipates the $\Delta\psi$. Known amounts of oxygen were added as small volumes of air-saturated water, which resulted in enzyme turnover. Proton ejection to the outside of the vesicles (sphaeroplasts) was detected by a sensitive pH-meter. The H^+/e^- pumping stoichiometry was calibrated by addition of anaerobic HCl of known concentration. The specific conditions used for pumping experiment in sphaeroplasts are described in ref [32], and for proteoliposomes in **Paper I** and **Paper III**.

4.3 Flash-photolysis measurements

Incubation of oxidized cytochrome *c* oxidase with carbon monoxide in an anaerobic environment results in formation of the $2e^-$ reduced, mixed-valence state (COMV). Binding of CO to heme a_3 of the binuclear center increases its midpoint potential and traps heme a_3 and Cu_B in a reduced state, while heme *a* and Cu_A are oxidized. Upon laser flash mediated photolysis of CO, the apparent midpoint redox potential of heme a_3 decreases. The electron situated at heme a_3 quickly redistributes to heme *a* followed by electron equilibration to Cu_A. The redistribution of electrons between the redox centers of cytochrome *c* oxidase can be time-resolved by optical spectroscopy using a single-wavelength spectrophotometer as described in ref [54]. From the obtained data, the rate of electron transfer between heme a_3, heme *a* and Cu_A can be extracted, as well as information of their relative midpoint potentials. See **paper IV** for experimental conditions.

4.4 Time-resolved optical and electrometrical flow-flash measurements

The flow-flash technique, invented by Gibson and Greenwood in 1963 [157], enable us to optically detect and distinguish different intermediates of the catalytic cycle of cytochrome *c* oxidase. As previously mentioned, the reaction between reduced cytochrome *c* oxidase and O_2 is very rapid. This means that when enzyme and oxygen is mixed together in a normal stopped-flow apparatus, the first steps of the oxygen reaction will be over already during the dead time of the instrument. This obstacle can be circumvented by the flow-flash technique, where reduced and CO-inhibited cytochrome *c* oxidase is mixed with excess O_2 in the dark. A strong laser pulse is thereafter used to dissociate CO from the enzyme. The reduced enzyme molecules will now bind O_2, and the oxygen reaction will simultaneously start in all cytochrome *c* oxidase molecules present. The oxygen reaction can be recorded optically at the wavelength of choice. For experimental details see **paper IV**.

A combination of the flow-flash technique with measurements of electric potential generation was developed by Drachev and co-workers in 1974 [158]. The electrometric flow-flash technique has been successfully applied in Helsinki Bioenergetics Group and has been thoroughly described by Jasaitis *et al*. [137]. In brief, the proteoliposomes containing reconstituted cytochrome *c* oxidase are attached to one side of a lipid-impregnated Teflon membrane, which separates two secluded compartments of the electrometric cell. The enzyme is thereafter degassed, reduced and kept CO inhibited in the dark. The oxygen reaction starts when an oxygen-saturated buffer is injected very close to the vesicles followed by flash photolysis of CO. The generation of electric potential during enzyme oxidation, i.e. the movement of electrons, protons and/or charged amino acid residues, can be kinetically resolved as a voltage change by Ag/AgCl electrodes positioned on separate sides of the Teflon membrane. The voltage detected by the electrodes is proportional to the voltage generated over the proteoliposome membrane. The experimental conditions used are described in **Paper IV**.

4.5 The reaction of cytochrome *c* oxidase with H_2O_2

The reaction between oxidized cytochrome *c* oxidase and H_2O_2 produces species equivalent to the $\mathbf{P_M}$ and **F** intermediates of the catalytic cycle. The product of the reaction depends on the pH of the medium (see chapter 5.5). In **paper IV**, cytochrome *c* oxidase in 100 mM MES, pH 6.5 or CHES, pH 9.5, supplemented with 0.02% DM was reduced with a small concentration of dithionite and kept in an oxygen free environment under constant nitrogen flow, in one chamber of a stopped-flow apparatus (Unisoku Instruments, Kyoto, Japan). The fully reduced cytochrome *c* oxidase was then mixed in a 1:1 ratio with aerated buffer containing 20 mM H_2O_2. Instantly upon mixing, the oxygen in the second chamber consumed the excess dithionite and oxidized the enzyme, resulting in an activated cytochrome *c* oxidase. Shortly thereafter, the freshly oxidized enzyme reacted with H_2O_2 present in the same solution. The absorption changes that followed were recorded using a diode array kinetics spectrophotometer (Unisoku Instruments).

4.6 Transmittance and attenuated total reflection FT-IR spectroscopy

Fourier transform infrared spectroscopy (FT-IR) detects vibrational motions within the chemical bonds of a molecule, by measuring the change in intensity of the infrared light before and after it interacts with the sample. The collected FT-IR spectrum of a biomolecule provides information about the protein secondary structure and structural interactions, and can even pinpoint specific bond vibrations. The CO photolysis difference FT-IR spectroscopy exploited in **paper IV** detects changes in bond vibrations of cytochrome *c* oxidase, which occur when CO bound to the reduced Fe_{a3} is dissociated and transiently binds to Cu_B. Comparison between CO difference FT-IR spectra of WT at different pH values or of WT and specific cytochrome *c* oxidase mutants can reveal changes in the structural conformation of the binuclear center or for example changes in hydrogen bonding or protonation state of specific functional groups within the enzyme. The experimental protocol for the FT-IR measurements in **paper IV** was essentially as described in ref [86].

Attenuated total reflection (ATR) FT-IR spectroscopy is a technique, which enables fast collection of IR spectra with a good signal-to-noise ratio from only a few micrograms of protein. In addition, the ATR FT-IR technique allows variations of the pH, salt

concentration or redox-conditions during the measurement. The infrared beam in the ATR FT-IR measurement is directed onto a silicon microprism of high refractive index (SensIR Technologies), on top of which the studied protein sample is applied. Above a critical angle, the light beam is totally reflected from the surface of the ATR microprism, and an evanescent wave is established at the interface between the prism and the protein sample. Formation of a dehydrated protein film on top of the silicon microprism was in **paper IV** insured by removal of detergent from the enzyme sample essentially according to Iwaki *et al*. [132]. After application on top of the microprism, the enzyme was gently dried using a flow of nitrogen. Once a stable protein film had formed, the enzyme was rewetted with 200 mM potassium chloride and 200 mM potassium phosphate, pH 6.5 and covered with a protecting lid. The lid is equipped with in and out ports, which allows a constant flow of buffer on top of the sample. In the experiment performed in **paper IV**, cytochrome *c* oxidase was oxidized by a buffer containing 1 mM ferricyanide and thereafter reduced by a buffer containing 3 mM anaerobic dithionite, in repeated cycles, to improve the signal-to-noise ratio of the measurement. The redox state of the enzyme was monitored throughout the experiment via an optical fiber connected to the lid, which covers the sample (DH-2000, Micropak and Oceans Optics Inc.). The resulting reduced-minus-oxidized difference FT-IR (detected by a Bruker ISF 66/S spectrometer equipped with a liquid nitrogen-cooled MCT-A detector) spectra may provide information about changes in bond vibrations, which occur upon transition between the oxidized and reduced state of cytochrome *c* oxidase.

4.7 Molecular dynamics simulations

Molecular dynamics (MD) simulations provide an efficient tool for theoretical time-dependent studies of conformational changes and thermodynamics of biological molecules. The MD simulations in **paper I** and **paper III** were performed using the AMBER force field and program (AMBER99, University of California, San Francisco [159,160]) after energy minimization of the bovine cytochrome *c* oxidase structure (PDB entry 1OCC, [22] and 1V54 [93]). For a detailed description of the simulation see **paper I** and **paper III**.

5. RESULTS AND DISCUSSION

5.1 The role of Glu278 in water-mediated proton transfer

5.1.1. Heme-copper oxidases can have alternative proton-conducting pathways

Collective experimental data have established that Glu278 has an essential role in oxygen reduction and proton translocation by cytochrome *c* oxidase [88,89,161]. Yet, Glu278 is not a totally conserved residue among the family of heme-copper oxidases (see chapter 1.2). There are examples of oxidases that lack an equivalent of Glu278, which nevertheless pump protons across the membrane [162-164]. These include heme-copper oxidases that lack most of the conserved residues of the D- and K-pathways of cytochrome *c* oxidase. Clearly, alternative proton conducting pathways must exist in these heme-copper oxidases or, more unlikely, these oxidases translocate protons across the membrane by a different mechanism from the mitochondrial-like cytochrome *c* oxidases (discussed in chapter 5.7.2). Three examples of heme-copper oxidases with modified proton pathways relevant to the present study are briefly described below.

The first example is the proton pumping caa_3 oxidase from *Rhodothermus marinus* (*R. marinus*), which has a high sequence homology with the cytochrome *c* oxidase from *P. denitrificans.* All key residues of the K- and D-pathways are conserved, with the only exception of Glu278 in helix VI [165]. According to a homology model between subunit I of the *R. marinus* caa_3 and *P. denitrificans* aa_3 oxidases, the phenol group of a tyrosine in the caa_3 oxidase occupies the same spatial position as the carboxylic side chain of Glu278 in the aa_3 oxidase [165]. The tyrosine is the only protonatable residue close to the position of Glu278 in *P. denitrificans* and was proposed to be involved in proton translocation by the *R. marinus* caa_3 oxidase [165]. An additional structural difference between the *R. marinus* and *P. denitrificans* oxidases is found at the position of a conserved glycine (Gly275) located three residues upstream from the Glu278 locus in the aa_3 oxidase. The glycine at this locus is substituted by a serine in the caa_3 oxidase from *R. marinus*. The structural combination of a tyrosine and a serine (a YS motif) close to the binuclear center instead of a glutamate

seems to be a general feature within the A2-subgroup of heme-copper oxidases, which the caa_3 oxidase from *R. marinus* represents.

Another example of a heme-copper oxidase that differs substantially from the main group of heme-copper oxidases with respect to its proton pathways is the ba_3 oxidase from *Thermus thermophilus* (*T. thermophilus*) [166]. The ba_3 oxidase has a very low sequence identity with the canonical oxidases (less than 20%) [167], and most of the amino acid residues common to the D- and K-pathways of cytochrome *c* oxidase are absent in the ba_3 oxidase. The atomic structure of the ba_3 oxidase from *T. thermophilus* was solved in 2000 [166]. The crystal structure shows the presence of three possible proton pathways, which consist of polar residues and crystallographically detected water molecules and lead from the N-side of the membrane to the vicinity of the binuclear center [166]. The ba_3 oxidase translocates protons across the membrane during catalytic turnover [163]. The reported proton pumping efficiency of the *T. thermophilus* ba_3 oxidase is though lower than for cytochrome *c* oxidase (~0.5 H^+/e^-), which has led to the speculation of a diverging proton pumping mechanism in the ba_3 oxidase [163].

The third example of a heme-copper oxidase with modified proton pathways is the aa_3 quinol oxidase from *Acidianus ambivalens* (*A. ambivalens*), which was studied in **paper II**. *A. ambivalens* is a thermoacidophilic archaeon, which expresses only one terminal oxidase, the aa_3 quinol oxidase [168]. Investigation of its amino acid sequence shows that most of the conserved residues of the K- and D-pathways of the cytochrome *c* oxidase are absent in the aa_3 quinol oxidase [169]. In **paper II**, the isolated quinol oxidase from *A. ambivalens* was reconstituted into vesicles and shown to pump 1 H^+/e^- across the membrane. At present, no crystal structure of the aa_3 quinol oxidase is available. Sequence alignment and structural homology modeling was therefore explored to find possible functional substitutions of the non-existing D-pathway residues in the aa_3 quinol oxidase (**paper II**). Based on a 3D model, a glutamate (Glu80 in *A. ambivalens*) was found in helix II of the aa_3 quinol oxidase, which is located near to the position of Glu278 in *P. denitrificans*. Although Glu80 (*A. ambivalens* numbering) is located further way from the binuclear center than Glu278 it could functionally substitute the latter and take part in proton transfer from the bulk phase to the binuclear center via water molecules. The locus that corresponds to Glu80 in *A. ambivalens* is in cytochrome *c* oxidase from *P. denitrificans* and *R. sphaeroides* occupied by an isoleucine (Ile104). Mutation of this isoleucine to a glutamate in aa_3 oxidase from *R.*

sphaeroides in the background of a Glu278 to alanine mutation (the double mutant E286A/I112E in *R. sphaeroides*) has been done to mimic the structure of the aa_3 quinol oxidase from *A. ambivalens* [170]. The resulting *R. sphaeroides* mutant retain the capability to translocate protons although the turnover activity was lowered substantially [170]. This supports the idea that Glu80 (*A. ambivalens* numbering) can functionally replace Glu278 as part of an alternative proton pathway in the aa_3 quinol oxidase from *A. ambivalens*.

5.1.2 Glu278 is not required for proton translocation by cytochrome *c* oxidase

For a long time Glu278 has been considered an essential amino acid for the function of cytochrome *c* oxidase [88,89,161]. Its carboxylic side chain is expected to rotate from a downward position, where it is in contact with the D-pathway, to an upward position towards the binuclear center during proton transfer [70,85,92]. The intriguing observation that some proton pumping heme-copper oxidases like the caa_3 oxidase from *R. marinus* are short of an equivalent of Glu278 close to the binuclear center challenged this view. In **paper I,** we performed site-directed mutagenesis on cytochrome *c* oxidase from *P. denitrificans* in order to find out how essential Glu278 is for the function of cytochrome *c* oxidase and whether it could be functionally substituted by another residue or alternatively several residues. The structure of cytochrome *c* oxidase in the area around Glu278 was changed to mimic that of the caa_3 oxidase from *R. marinus*. Based on the sequence alignment (Figure 7), Glu278 was mutated to an alanine, Gly275 to a serine and Phe274 to a tyrosine, both as single mutations and in different combinations. The E278A mutation alone rendered the enzyme highly inactive (~1% of WT activity) and abolished proton translocation, in agreement with previously published data [161]. Exchange of Gly275 to a serine resulted in a drastically lowered catalytic activity (~3% of WT) and inhibition of proton translocation. One possible explanation for the observed effects in the G275S mutant is that the hydroxyl group of Ser275 interacts with the side chain of Glu278 at its putative upward position and affects its ability to conduct protons. Gly275 is situated at a narrow point of a possible O_2 channel, which intersects the hydrophobic cavity located between Glu278 and the binuclear center [28]. Mutation of Gly275 to a valine in the aa_3 oxidase from *R. sphaeroides* has been reported to limit the access of O_2 to the active site [171]. Another explanation for the low oxygen consumption activity in the G275S mutant can thus be that the mutation has affected the access of O_2 to the binuclear center.

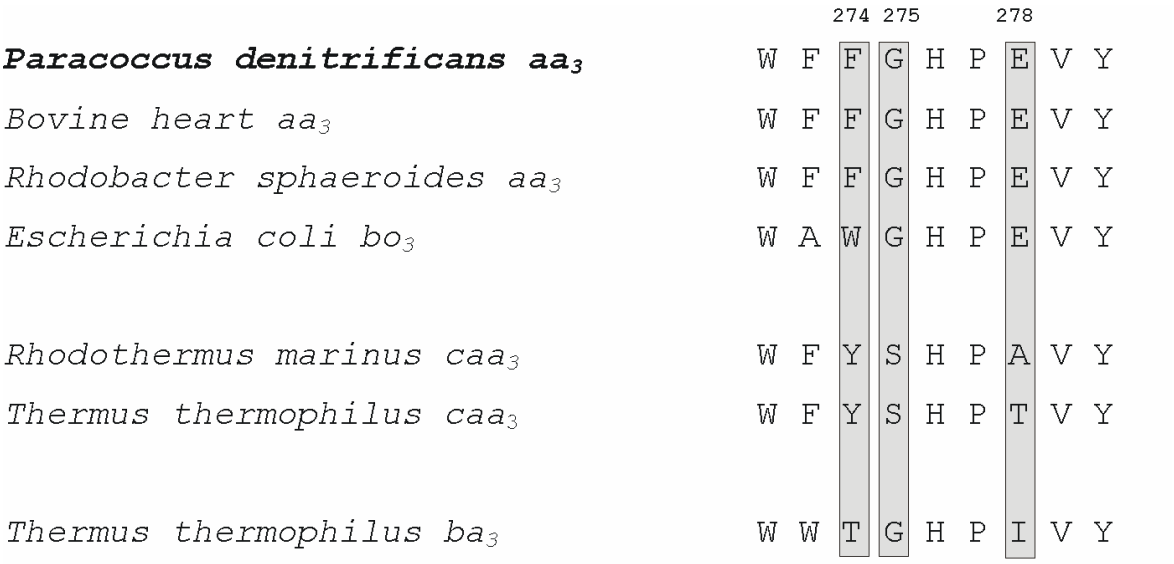

Figure 7. Sequence comparison between cytochrome aa_3 from *P. denitrificans* and other representatives of the A1-subgroup of heme-copper oxidases, with oxidases from the A2-subgroup and the B-type of heme-copper oxidases (see chapter 1.2). The highly conserved Glu278 found in *P. denitrificans* is substituted by an alanine in *R. marinus* caa_3, a threonine in *T. thermophilus* caa_3 and an isoleucine in *T. thermophilus* ba_3. Moreover, Phe274 and Gly275 in *P. denitrificans* are substituted by other amino acid residues in the distantly related heme-copper oxidases.

When the two single mutants are combined into a double mutant, G275S/E278A, a stable enzyme is formed with practically no oxygen reducing activity (<0.1% of WT activity). Clearly, the small remaining activity in the single mutations strongly depends on the presence of the other amino acid. Introduction of a tyrosine at the Phe274 locus into the G275S/E278A double mutant (i.e. the triple F274Y/G275S/E278A mutant) has astonishing effects. The triple mutant, which mimics the structure of the caa_3 oxidase from *R. marinus*, has ~10% of WT activity and translocates protons across the membrane with WT-like efficiency (**paper I**). The triple mutant is the first example of a non-conservative mutation at the Glu278 locus, which sustains proton-pumping ability. Previously, only a very conservative mutation of Glu278 to an aspartate maintained proton pumping by cytochrome *c* oxidase [89]. The general assumption was therefore that a carboxylic acid is essential at the 278 locus in order for cytochrome *c* oxidase to pump protons. This is clearly not the case. Introduction of a hydrogen-bonding amino acid at a key position in the structure seems to be enough to maintain the proton pumping capability. In **paper I** and **II** we show that in fact several alternative structural solutions in the area around Glu278 can support proton transfer in cytochrome *c* oxidase. These include in addition to the triple mutant, a

F274T/E278I motif, which mimics the ba_3 oxidase from *T. thermophilus* [166] and a F274Y/G275S/E278T motif, which mimics the caa_3 oxidase from *T. thermophilus* [164] (Figure 7). The implications of these results on the general mechanism whereby heme-copper oxidases translocate protons are discussed in chapter 5.7.2.

The structural basis for proton translocation by cytochrome *c* oxidase in the absence of Glu278 was studied in the triple mutant, F274Y/G275S/E278A, by molecular dynamics (MD) simulations (**paper I**). The area between Glu278 and the binuclear center is, as previously mentioned, hydrophobic and does not contain any structurally detected water molecules. In addition, it is proposed to be part of a channel for O_2 diffusion to the active site [28,39]. Still, at least a transient presence of water molecules in the hydrophobic cavity is very likely, since a constant production of water molecules occurs at the binuclear center. The presence of water molecules in the cavity is supported by theoretical calculations as well as FT-IR spectroscopy [70,85-87,172,173]. Our MD simulations with the triple mutant included consequently six theoretically predicted water molecules [85]. A model of the triple mutant structure was made based on the 3D structure of bovine cytochrome *c* oxidase (PDB entry code OCC, ref. [27]) and subjected to energy minimization. An area with a diameter of approximately 15 Å around Tyr274 was then used in the MD simulations (**paper I**).

The MD simulations started with a one picosecond (ps) equilibration at 150 K followed by 100 ps at 300 K. Within 3 ps of the start of the MD simulations, a transient hydrogen-bonded water chain was formed, which connected Ser193 in end of the D-pathway to the binuclear center and lasted for the whole duration of the simulation (**paper I**). The four water molecules present in the cavity between Tyr274 and His326, one of the ligands of Cu_B, repositioned themselves so that a hydrogen-bonded connection was formed between Tyr274 and the Nε of His326. In addition, the two water molecules present between Tyr274 and Ser193 in the end of the D-pathway linked the serine to Tyr274. In this way, a long chain of water molecules was formed that is anchored by the OH group of Tyr274. Formation of the water chain depends critically on support from the structure. No corresponding chain of water molecules was formed in control simulations with the WT enzyme, where Glu278 is situated with its carboxylic side chain pointing downwards. Results similar to ours have recently been reported from independent MD simulations of the F274Y/G275S/E278A triple mutant by Sharpe and co-workers [174]. In their simulations,

Tyr274 is positioned with its phenol group in hydrogen bonding distance to a water molecule [174].

The distance between Tyr274 and the closest proton acceptor on the exit side of cytochrome *c* oxidase is approximately 10 Å. Due to the large separation in space, it is inconceivable that protons could be transferred to the active site without the recruitment of water molecules. The phenol group of tyrosine has a pK_a of ~10.5 in an aqueous solution. The pK_a value of Tyr274 is expected to be higher due to the hydrophobic environment that surrounds the residue [73,175]. A high pK_a value would disfavor deprotonation of Tyr274 in the triple mutant and Tyr274 might instead merely stabilize water molecules involved in proton transfer. Transient deprotonation of Tyr274 during catalytic turnover cannot still be excluded. A recent FT-IR spectroscopy study of the *R. marinus caa*$_3$ oxidase suggests that a tyrosine residue is deprotonated upon formation of the $\mathbf{P_M}$ intermediate of the catalytic cycle [176]. The authors suggest that the deprotonated tyrosine is the functional counterpart of Glu278 in *R. marinus*, i.e. equivalent to Tyr274 in our simulation.

The MD simulations with the F274Y/G275S/E278A triple mutant showed that proton transfer from the end of the D-pathway to the binuclear center is mediated through a six-membered hydrogen-bonded water chain, which is supported by the OH group of Tyr274. In WT enzyme, the presence of Glu278 instead of Tyr274 will effect the local environment differently. Glu278 is on the contrary to Tyr274 an acidic residue. This property may divide the proton-conducting path between the D-pathway and the binuclear center into two separate entities and favor independent formation of two shorter water chains. A water chain consisting of only a few molecules will form with much higher probability that one with several contributing water molecules. The location of Glu278 in between two short water stretches may improve the rate and probability of proton transfer in cytochrome *c* oxidase. It is feasible, that Glu278 will function as an actual proton donor and acceptor between these separate water chains, whereas Tyr274 will merely stabilize the formation of a longer water chain.

5.2 Arg473 and the Δ-propionate of heme a_3 regulate the access of pumped protons to the P-side of the membrane

The identity of the primary acceptor of pumped protons on the output side of the membrane is still disputed. A FT-IR spectroscopy study indicates that at least two out of the four heme propionates change their protonation state or experience changes in their hydrogen bonding environment upon reduction of the hemes [177]. It was proposed that the Δ-propionate of heme *a* is the group that will accept a proton when cytochrome *c* oxidase is reduced, while the Δ-propionate of heme a_3 was suggested to change its conformational state or possibly act as a proton donor [96]. The report is contrasted by a mutagenesis study, which indicates that the primary proton acceptor of pumped protons is the Δ-propionate of heme a_3 [91,151,178].

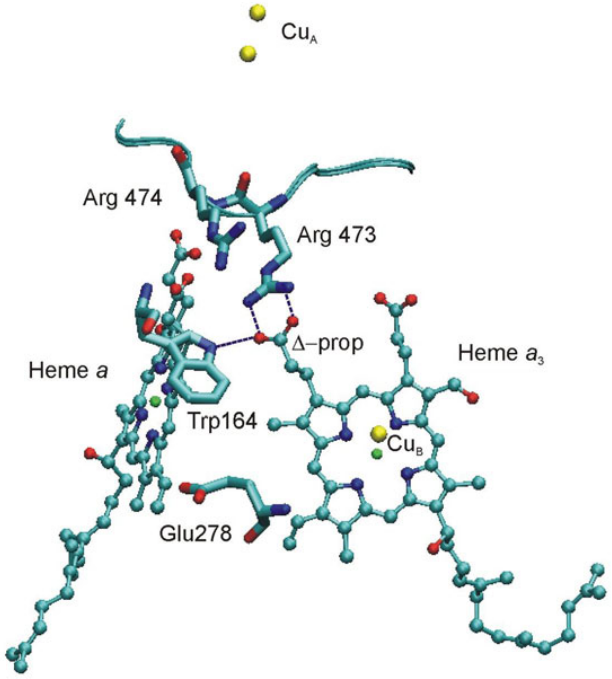

Figure 8. The redox-active centers of cytochrome *c* oxidase and key amino acids in the area surrounding the Δ-propionate of heme a_3 (PDB entry code 1AR1, [21]). The heme a_3 Δ-propionate is hydrogen bonded to Trp164 and Arg473, and is stabilized in its anionic state by charge interactions with Arg473 and Arg474. The picture was prepared using the VMD software [35].

The heme a_3 Δ-propionate is stabilized in its anionic state by charge interactions with Arg473 and Arg474, and through hydrogen bonds to Arg473 and Trp164 (Figure 8). The close distance between Arg473 and the Δ-propionate of heme a_3 in the static crystal structure implies that a strong electrostatic interaction exists between these two. The high stability of such an ion bond has been used as an argument that the propionate cannot accept a proton [93]. The existing 3D structures are however merely snap-shots of the enzyme and cannot reveal structural fluctuations that may occur during catalytic turnover. We therefore decided to investigate the stability of the ion pair between Arg473 and the heme a_3 Δ-propionate using MD simulations (**paper III**).

Our MD simulations included most of subunit I and II as well as four water molecules that were modeled into the hydrophobic cavity near the binuclear center. Cu_B was ligated by a hydroxide, and Asp399 and Glu278 were protonated whereas all heme propionates were deprotonated. The simulation was set up to mimic electron transfer from heme *a* to the binuclear center in such a way that heme *a* was initially reduced whereas the binuclear center was oxidized, followed by the opposite redox configuration. The resulting system was very stable, with very small variations in interatomic distances. Yet, one thermal fluctuation was noteworthy. The hydrogen-oxygen distance (2HH2-O2D) between Arg473 and the Δ-propionate of heme a_3 oscillated transiently from its equilibrium position of about 2 Å to more than 4 Å (**paper III**). The complete oscillation from opening of the arginine/Δ-propionate ion pair until it returned to its initial position lasted 0.4-0.8 ps. In the MD simulations the ion pair was fully dissociated, defined as a separating distance of more than 4 Å, for approximately 0.1 ps. According to quantum mechanical simulations with bacteriorhodopsin, proton transfer via a preformed water path can occur through a Grotthuss-type of mechanism with a rate of 0.05 ps [179]. The thermal fluctuation of the arginine/Δ-propionate ion pair exhibited a strong dependence on the redox-state. It occurred only when the water molecules in the hydrophobic cavity connected Glu278 with the propionate (i.e. heme *a* reduced/binuclear center oxidized). No fluctuation of the distance was observed in the absence of water molecules in the cavity or when the hydrogen bond from Trp164 was removed [151]. Destabilization of the ion pair will thus depend both on a specific dipole moment of the water molecules in the cavity, as well as the hydrogen bond from Trp164.

The MD simulations were verified experimentally by proton translocation experiments with the Trp164 to phenylalanine mutant in *P. denitrificans* (**paper III**). By this mutation the hydrogen bond to the Δ-propionate of heme a_3 is abolished. As a result, the proton pumping stoichiometry of the W164F mutant decreased to about ~0.5 H^+/e^- compared to 1 H^+/e^- in WT. The data show that Trp164 has a role in proton pumping by cytochrome *c* oxidase. The W164F mutant was though able to translocated protons across the membrane with about half of WT efficiency. This implies that the hydrogen-bonded water chain present in the cavity between heme *a* and heme a_3 is the primary modulator of the stability of the ion pair between Arg473 and the heme a_3 Δ-propionate.

We suggest that the Arg473/Δ-propionate ion pair is the long-sought gate that regulates the access of protons between the P- and N-side of the membrane. Dissociation of the ion pair is likely to raise the pK_a of the propionate considerably. We may envision one of the following scenarios. The raised pK_a of the propionate will attract a proton from Glu278, which is transferred via the hydrogen-bonded water chain that connects Glu278 to the Δ-propionate. The arriving proton will raise the electron affinity of heme a_3, resulting in fast eT from heme *a* to the binuclear center, which will ultimately trap the proton at the propionate. In the other scenario, the Δ-propionate is transiently protonated by the proton arriving from Glu278. Simultaneously, Arg473 releases a proton to an acceptor (the pump site) located somewhere above the hemes. The ion pair is thereafter renewed when the proton residing of the propionate is moved to the arginine. Reduction of the binuclear center will reorientate the water dipoles in the hydrophobic cavity so that a hydrogen-bonded link is formed between Glu278 and the active site. Glu278, which have been reprotonated via the D-pathway, will then donate a substrate proton to the binuclear center. As a consequence, the proton at the Δ-propionate or the alternative pump site will be expelled to the P-side of the membrane through electrostatic repulsion. A role for the Δ-propionate of heme a_3 and Arg473 in proton translocation by cytochrome *c* oxidase has recently been supported by several papers [178,180,181].

5.3 The influence of water molecules on the open and closed state of the Arg473/heme a_3 Δ-propionate gate

More than 600 water molecules per second are produced at the active site of cytochrome *c* oxidase during catalytic turnover. The exit of these product water molecules to the bulk phase must be controlled in both time and space. Free diffusion of water could be devastating for cytochrome *c* oxidase by allowing uncontrolled proton leakage across the membrane [63,65]. Both experimental and computational data have shown that the water molecules produced at the binuclear center are fundamental for the proton-conducting mechanism [70,85,87,151] (**paper I**). The water molecules may also be involved in the regulation of different electron transfer steps within the enzyme [182]. The removal of product water molecules is hence of key importance when the function of cytochrome *c* oxidase is considered.

The exit of product water molecules to the P-side of the membrane occurs via the Mg^{2+} site, which is located above the binuclear center [27]. EPR studies using labeled O_2 and D_2O have shown that the Mg^{2+} site is in rapid equilibrium with the external water phase [30] as well as with the binuclear center [102]. Most likely, the water molecules exit via a specific pathway, although such a path leading from the binuclear center to the Mg^{2+} site has not yet been localized.

Our MD simulations revealed that the ion pair formed by Arg473 and the Δ-propionate of heme a_3 can function as a gate, which regulates proton access between the different sides of the membrane (**paper III)**. In addition to this, the MD simulations shows that when an additional water molecule is added to the cavity between the hemes (a total of five H_2O molecules) the gate opens and a water molecule located in the cavity can escape towards the Mg^{2+} site and from there on presumably towards the P-side of the membrane. Removal of the crystallographically detected water molecules above the hemes also trigger opening of the gate and allows a water molecule to exit the cavity. However, with no water molecules present in the cavity, the Arg473/propionate gate remains shut.

As previously mentioned, dissociation of the ion pair critically depends on the dipole moment of the water molecules in the cavity, which is determined by the redox-state of the hemes. An excess of water molecules in the cavity results however in opening of the

Arg473/Δ-propionate gate that is not controlled by the redox state of the hemes. This scenario is most unwanted, since opening of the gate in a state where heme *a* is oxidized and the binuclear center is reduced, could lead to backleak of protons from the outside to the binuclear center.

Mutation of Arg473 to a lysine results in an enzyme with proton pumping efficiency and catalytic activity under steady-state conditions that is equal to WT enzyme [183]. In the presence of a membrane potential the turnover activity of the R473K mutant decreases substantially in comparison with WT. The low activity in the presence of an electrochemical gradient can be interpreted as a decrease in the rate by which protons leak from the P-side of the membrane to the binuclear center. Recent MD simulations indicate that exchange of Arg473 to a lysine will increase the positive charge density around the Δ-propionate of heme a_3 [180]. A change in the electrostatic charge distribution can lead to a more tightly shut arginine/propionate ion pair in the R473K mutant, which would explain the decrease in proton leakage from the P-side of the membrane.

The proton affinity of the group(s) that regulates proton backleak into cytochrome *c* oxidase appears also to be affected by the W164F mutation (**paper IV**). The amplitude of electric potential generated across the membrane when fully reduced WT cytochrome *c* oxidase in vesicles reacts with O_2 is pH dependent. In alkaline conditions, a decrease in amplitude is detected, which is not caused by an increase in the proton permeability of the liposomes, and which is reversed when the pH is lowered. The decrease in generated amplitude in high pH conditions in WT can be explained by leakage of protons from the P-side of the membrane [183]. The pH dependence can be fitted to an apparent pK_a of ~9.9. Interestingly, the W164F mutant exhibits a different pH dependence of the generation of electric potential from that of WT (**paper IV**). In the mutant the decrease in the amplitude of membrane potential appears already at a lower pH. The pH dependence for the W164F mutant can be fitted to an apparent pK_a of ~9.0. The result can be interpreted as a decrease in the apparent proton affinity of the group(s) that regulates proton leakage from the P-side of the membrane caused by the W164F mutation. The MD simulations in **paper III** showed that the hydrogen bond between Trp164 and the Δ-propionate of heme a_3 is an important factor that regulates the stability of the Arg473/Δ-propionate ion pair. We can therefore speculate that opening of the Arg473/propionate gate occasionally allows leakage of protons back to the binuclear center, especially at high pH conditions. A controlled backleak of protons from the outside to the binuclear center has been proposed to regulate the efficiency

of energy transduction by cytochrome *c* oxidase [183]. Our MD simulations indicate that the proton leakage is ultimately controlled by the activity and presence of the water molecules in the hydrophobic cavity between the hemes. In simulations where the water molecules in the cavity were removed, the Arg473/propionate gate remained firmly shut.

5.4 The reprotonation rate of Glu278 is affected by the W164F mutation

Glu278 functions as the immediate proton donor to either the binuclear center or the pump site six times during one catalytic turnover. Upon deprotonation Glu278 is normally quickly reprotonated via the D-pathway. Certain mutations in the D-pathway, such as the D124N mutation at the entrance of the channel, will however block proton transfer and ultimately lead to slowed or inhibited reprotonation of Glu278 [136]. It has been shown that the partial oxidation of Cu_A during $\mathbf{P_R \rightarrow F}$ transition depends on proton uptake to Glu278 through the D-pathway [88,135].

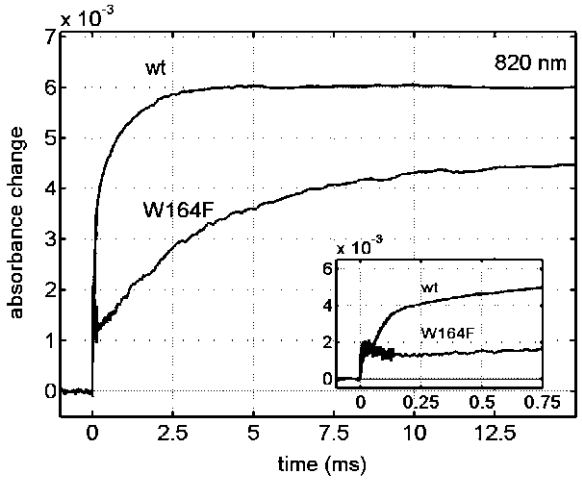

Figure 9. The flow-flash reaction of fully reduced WT and W164F cytochrome *c* oxidase with oxygen recorded at 820 nm, which is the optimal wavelength for detection of oxidoreduction of Cu_A. The traces are normalized to the total enzyme concentration. The inset shows the absorption changes that occur during the first 750 μs after the enzyme has been allowed to react with O_2.

In **paper IV**, the rate of oxidation of the Cu_A center in the W164F mutant was investigated by time-resolved optical flow-flash and compared to WT cytochrome *c* oxidase. In WT, the initial formation and decay of intermediate **A** is followed by a biphasic increase in absorbance at 820 nm (Figure 9). The first phase (τ ~50 μs) corresponds to the partial oxidation of Cu_A by heme *a* during the $\mathbf{P_R \rightarrow F}$ transition, whereas the second (τ ~1 ms) corresponds to the final oxidation of Cu_A upon the complete oxidation of the enzyme. In the

W164F mutant (Figure 9), the fast electron equilibration between heme *a* and Cu_A was absent and only a much slower Cu_A oxidation was detected (τ ~3.5 ms).

A decrease in the rate of Cu_A oxidation in the W164F mutant was confirmed by flow-flash measurements at 445 nm (**paper IV**). At this wavelength, re-reduction of heme *a* by Cu_A is observed in WT as a plateau in the absorption (τ ~60μs), whereas no corresponding phase of heme *a* reduction was detected in the W164F mutant. A decrease in the rate of electron transfer from Cu_A to heme *a* can be caused by a shift in the redox equilibrium between heme *a* and Cu_A (however see below). The rate and extent of eT between the different redox centers of cytochrome *c* oxidase will depend on the relative midpoint potentials of these centers. In W164F, electron backflow experiments together with an investigation of the rate of CO recombination to the enzyme reveal that the E_m of heme a_3 has decreased by ~50 mV compared to WT. Backflow experiments did not indicate any change in the E_m of neither heme *a* nor Cu_A. We therefore interpret the effect of the W164F mutation on the rate of Cu_A oxidation as a decrease in the rate whereby Glu278 is protonated via the D-pathway (**paper IV**). Such an effect could be expected if the mutated residue resided in the D-pathway below Glu278. Trp164 is however located approximately 5 Å to the P-side of Glu278. The carboxylic side chain of Glu278 points down towards the entrance of the D-pathway in the resolved X-ray structures. Both experimental and theoretical data have however implied that the side chain rotates to an upward position in order to fast deliver protons for both chemistry and pumping [70,85,92] (and see **paper I)**. In our opinion, the effect of the W164F mutation on the reprotonation rate of Glu278 seems very unfeasible without rotation of the side chain of Glu278. The benzoid ring of Phe164 is likely to take the same position as the pyrrol ring of Trp164. In doing so, additional space will appear near the upward position of the carboxylic side chain of Glu278. Small structural rearrangements may also appear in the area, as the enzyme adopts itself to a different amino acid composition. Changes like these may affect the hydrogen-bonding environment around Glu278. Indeed, comparison of the ATR FT-IR spectra of W164F and WT enzyme indicates that changes in the environment around Glu278 have occurred (**paper IV**). Most likely, Glu278 will favor a different conformation in the W164F mutant from that in WT enzyme. In this conformation Glu278 will not be in rapid contact with the D-pathway. These results indicate that the reprotonation rate of Glu278 in cytochrome *c* oxidase is not only determined by the availability of protons from the D-pathway. It also depends highly on the correct conformation of Glu278.

5.5 The reaction of oxidized cytochrome c oxidase with H_2O_2

The reaction between oxidized cytochrome *c* oxidase and H_2O_2 produces intermediate states of the binuclear center, which can be recognized by their characteristic absorption spectrum [184-188]. When the reaction occurs at high pH (pH ~9) it results in the quick formation of the $\mathbf{P_M}$ intermediate (absorbing maximally around 609 nm), which thereafter decays into the **F** intermediate (absorbing maximally around 580 nm). In low pH (pH ~6.5), a mixture of the $\mathbf{P_M}$ intermediate and an **F**-like intermediate is instantly formed, which eventually decays into the **F** intermediate. The relative extent of the two intermediates in the mixture is pH-dependent and titrated with an apparent pK_a of about 7 for WT cytochrome *c* oxidase from *P. denitrificans* (**paper IV**). Previously, the corresponding phenomenon in the bovine enzyme was described with an apparent pK_a of 6.7-7.3 [184,189]. The **F**-like intermediate is called **F´**or **F** or alternatively "fast **F**" and has an absorption maxima around 575 nm. The **F´** specie contains, on the contrary to the **F** intermediate, only two reducing equivalents in the binuclear center and is hence isoelectronic with $\mathbf{P_M}$. The **F´** and $\mathbf{P_M}$ intermediates are yet likely to differ in their Cu_B ligation, which is assumed to be a water molecule in **F´** and a hydroxide in $\mathbf{P_M}$.

When oxidized W164F enzyme is allowed to react with H_2O_2 a substantial amount of **F´** is formed also at high pH (pH 9.5) (**paper IV**). The apparent pK_a of the ratio between the $\mathbf{P_M}$ and **F´** intermediates is approximately 2 pH units higher for W164F compared to WT cytochrome *c* oxidase from *P. denitrificans*. Konstantinov and co-workers have reported that the pH dependence of the formation of $\mathbf{P_M}$ and **F´** is mediated from the N-side of the membrane [189] and can be abolished by mutations in the K-pathway [185]. It was shown that the reaction of the K354M mutant with H_2O_2 at low pH produces solely the $\mathbf{P_M}$ intermediate [185]. To explain this observation, Pecoraro and co-workers proposed a branched reaction scheme of the reaction between oxidized cytochrome *c* oxidase and hydrogen peroxide, where the $\mathbf{P_M}$ and **F´**states are not in rapid equilibrium [185] (see also [184,190]). According to Pecoraro and co-workers, the reaction between oxidized enzyme and hydrogen peroxide produces transiently a common "peroxy intermediate" ($\mathbf{P_O}$), from which two competing pathways lead to formation of either $\mathbf{P_M}$ or **F´**. The rate constant for formation of the **F´** intermediate is dependent of pH. One prerequisite of their model is that the observed pK_a of the $\mathbf{P_M}$/**F´** ratio is only apparent and is determined by the relative rates of the two competing reactions. Several weak points however exist in this reaction scheme.

Following the model of Pecoraro and co-workers, one has to assume that formation of $\mathbf{P_O}$ is the rate-limiting step in the reaction. The formation of $\mathbf{P_M}$ and **F´** must therefore be faster that the maximum rate of ~50 s^{-1} estimated for $\mathbf{P_O}$ formation based on the observed bimolecular reaction rate and the used H_2O_2 concentration [184,185]. If we assume a rate of 100 s^{-1} for the formation of $\mathbf{P_M}$, the proton-dependent rate constant for formation of **F´** has to be 10^9 $M^{-1}s^{-1}$ to give an apparent pK_a of ~7 for the relative amplitudes of $\mathbf{P_M}$ and **F´** formation. This appears quite fast for proton uptake through the K-pathway. Yet, splitting of the dioxygen bond with the formation of the $\mathbf{P_M}$ intermediate has a rate of more than 5000 s^{-1} [119], which means that a rate of only 100 s^{-1} for the formation of the $\mathbf{P_M}$ state is a clear underestimate. To explain the observed 2 unit increase in pK_a of the peroxide reaction in the W164F mutant the rate of formation of $\mathbf{P_M}$ would have to decrease 100 times due to the mutation.

In **paper IV**, we propose an alternative reaction model (**paper IV**, scheme 2) where the observed pK_a is real and reflects the pH dependence of the protonation of peroxide bound to heme a_3 (in the $\mathbf{P_O}$ state). At the start of the reaction, H_2O_2 binds to the binuclear center, which is ligated by two OH^- groups, one bound to Fe_{a3}^{3+} and the other to Cu_B^{2+}. A transient $\mathbf{P_O}$ intermediate is formed with the production of two water molecules and a deprotonated peroxide bridge ligating the iron and copper. If the bound hydroperoxide has a p*K*a of ~7, it may be protonated via the K-pathway at pH values ≤ 7, resulting in a transient pH-dependent mixture of peroxide and hydroperoxide bound to heme a_3. Upon breakage of the peroxide O-O bond, the bound peroxide will form $\mathbf{P_M}$ (with an OH^- bound to Cu_B) and the bound hydroperoxide will form **F´** (with an H_2O bound to Cu_B). Once heme a_3 is in the ferryl state, proton exchange between $\mathbf{P_M}$ and **F´** is no longer possible, since both products block the K-pathway [185]. In this scenario, the peroxide itself is the protonatable site that determines the outcome of the reaction. We have shown that the W164F mutation lowers the midpoint potential of heme a_3 (**paper IV**). It is therefore highly possible that the W164F mutation causes an increase in of the pK_a of the iron-hydroperoxide (Fea_3^{3+}-OOH) structure by two pH units. As a result, the hydroperoxide ligand dominates and the **F´** intermediate will be formed at pH values well above 7.

5.6 Loading of the pump site in the **A→P_R** transition

The electrometric technique is a powerful tool for studying charge translocation across the membrane in real time. In **paper IV**, the generation of membrane potential (ΔΨ) in the reaction of fully reduced W164F oxidase with oxygen was studied and compared to WT. The photo-dissociation of CO from the fully reduced WT cytochrome *c* oxidase in the presence of O_2, leads to instant (τ ~10 μs) formation of the oxygen adduct, intermediate **A**, followed by eT from heme *a* into the binuclear center, which breaks the O-O bond and generates **P_R** (τ ~20 μs). The initial steps **R→A→P_R** have been considered electrically silent and were assigned to the initial lag in the electrometic response [137]. A fast phase of membrane potential generation develops thereafter (τ ~50 μs), which corresponds to the optically recorded **P_R→F** transition. This step is electrogenically associated with the uptake of a substrate proton into the binuclear center and the simultaneous electron equilibration between Cu_A and heme *a*. In addition, the **P_R→F** transition is coupled to pumping of one proton across the membrane in WT enzyme. In the subsequent step, the **F→O** transition (τ ~200 μs and τ ~1.3 ms), a fourth electron is delivered to the binuclear center, which together with the arrival of a second substrate proton completes the oxygen chemistry. The **F→O** transition is also linked to pumping of one proton across the membrane in WT enzyme.

Two interesting features are observed when the electrometric response of the W164F mutant is compared to WT cytochrome *c* oxidases (Figure 10). First, the fast phase of membrane potential generation (τ ~100 μs) account for only ~12% of the total ΔΨ in W164F. This is in contrast to WT, where the generated electric potential is equally split between the **P_R→F** and **F→O** reaction steps. Second, the initial lag appears to be shorter for the mutant than for WT, corresponding to mean values of 12 and 30 μs, respectively. The double mutant D124N/W164F, in which the entrance of the D-pathway is blocked [82,83], has the same electrometric feature as the W164F single mutation, i.e. only ~12% of the total ΔΨ is generated in the fast electrometic phase. If a partial backleak of protons from the P-side of the membrane would occur in the W164F mutant it would, in combination with the D124N mutation, lower the amplitude of the fast phase further or even reverse its sign. The observed decrease in amplitude of the fast phase of the W164F mutant is therefore real and not an artifact of protonic leakage from the P-side of the membrane, which can occur at alkaline pH (see chapter 5.3). The amplitude of the fast phase in W164F corresponds to the

movement of one charge approximately 30% of the membrane dielectric (**paper IV**). The distance from the N-side of the membrane to the binuclear center corresponds to ~0.7 of the membrane dielectric. This means that the amplitude of the fast phase of W164F cannot account for the uptake of a substrate proton from the bulk solution to the binuclear center nor be associated with proton pumping across the membrane.

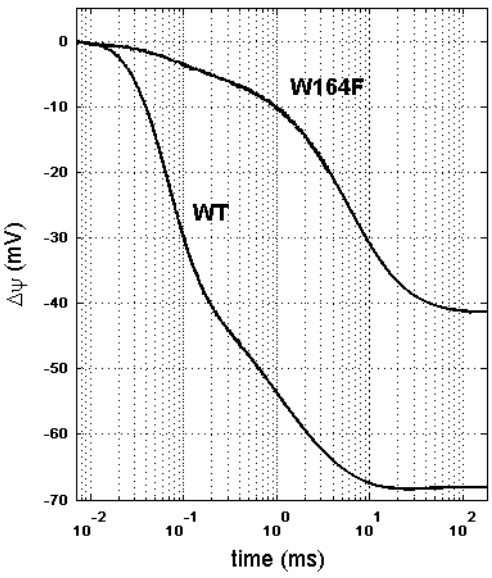

Figure 10. The generation of electric potential by WT and the W164F mutant after addition of oxygen to the fully reduced enzyme. At the start of the reaction, oxygen binds to the enzyme forming compound **A**, which is followed by splitting of the O-O bond and formation of compound $\mathbf{P_R}$. The first steps of the reaction ($\mathbf{R \rightarrow A \rightarrow P_R}$) have previously been attributed to the initial lag in the electrometric trace. Electric potential ($\Delta\Psi$) then develops in three phases in WT. The first phase equals the $\mathbf{P_R \rightarrow F}$ transition (τ ~50 μs) and constitutes ~50% of the total amplitude generated for WT (~70 mV). The second two phases equal the **F→O** transition in WT (τ ~200 μs and ~1.3 ms) and constitute together ~50% of total $\Delta\Psi$. In W164F, the first phase corresponds to only ~12% of the total $\Delta\Psi$ generated and has a time constant of ~100 μs. It is followed by two slower phases with time constants of 5-7 ms and 14-20 ms, which together constitute ~35 mV.

In order to determine the state of the binuclear center in each electrometric transition, time-resolved optical flow-flash of the fully reduced oxidase with O_2 was used. Optical changes at 580 nm are mainly associated with the appearance and decay of the ferryl intermediate **F** [118], but also reflect the kinetics of formation of intermediate **A** [191]. In the W164F mutant, intermediate **A** appeared at 580 nm with roughly the same kinetics as in WT, whereas the decay of **A**, which is normally associated with formation of $\mathbf{P_R}$, was approximately twice slower (**paper IV**). In WT, a subsequent increase in absorbance at 580 nm was detected (τ ~40 μs), which corresponds to the formation of the ferryl state of the binuclear center. No corresponding phase was detectable in W164F with the time-resolution of the flow-flash experiment. However, intermediate **F** eventually forms in the W164F mutant, albeit on a much slower time scale (>5 ms), since the final oxidation of the enzyme together with the decay of **F** is detected optically with a slower flow-flash measurement.

The optically detected decay of **F** in the W164F mutant (>5 ms) coincides with the development of two slow phases (τ ~5 ms and τ ~20 ms) in electrometry, which are associated with generation of Δψ of the same magnitude as in the **F→O** transition of WT. The slow phases of electric potential generation in W164F are likely to comprise many electrogenic events, i.e. a) the uptake of two substrate protons to the binuclear center, one for formation of the **F** state and one for **F→O** transition, b) electron transfer from Cu_A to heme *a* and c) uptake of proton(s) that are pumped across the membrane.

The results from the optical and electrometrical flow-flash experiments appear at first sight inexplicable. The fast phase of electric potential generation in the W164F mutant (in WT corresponding to $\mathbf{P_R}$**→F** transition) is only twice slower than WT. Yet, optically no **F** intermediate develops with the same kinetics. The logical conclusion is that the small fast electrometric phase does not include formation of the **F** intermediate, but reflects another vectorial charge translocation in the W164F enzyme. In WT, the amplitude of the fast phase ($\mathbf{P_R}$**→F** transition) includes a small contribution from the partial eT between Cu_A and heme *a*. The electron equilibration between Cu_A and heme *a* is dramatically slowed in the W164F mutant (Figure 9) and would not attribute to the fast electrometic response. In the fast optical flow-flash measurement, formation of the **F** state was not detected in the W164F mutant during the time-resolution of the experiment. This means that the fast electrometric phase in W164F precedes by far the formation of intermediate **F** in W164F. Part of the explanation for the decrease in amplitude is hence a lack of proton uptake into the binuclear center for the formation of **F**. Nevertheless, the origin of the small fast amplitude is W164F cannot be explained by this observation.

As previously mentioned, there is a large separation in time between the fast electrometric phase of W164F and the optically detected transition of $\mathbf{P_R}$ state to **F**. Moreover, the initial lag phase of membrane potential generation in W164F is shorter than in WT. When this is considered, the kinetics of the development of the initial amplitude in the W164F mutant actually coincides with the first step of the catalytic reaction in WT, the **A→**$\mathbf{P_R}$ transition.

$\mathbf{P_R}$ formation is associated with transfer of an electron from heme *a* to the binuclear center. This eT occurs in the plane of the membrane and does not contribute to the generation of membrane potential. Only electrons and protons that move perpendicular to the membrane will give rise to an electrometrically detectable signal. Since the oxidation of Cu_A in W164F has a time constant of milliseconds, it is safe to assume that no electron

transfer events occurs perpendicular to the membrane during the fast electrometric phase. Instead, the amplitude must originate from a vectorial proton transfer, which occurs simultaneously with the eT from heme *a* to heme a_3. A likely proton donor could be Glu278, which is known to be involved in the transfer of both chemical and pumped protons many times during enzyme turnover. The target of the proton transfer cannot be the binuclear center. Proton delivery to the active site would immediately yield the **F** intermediate, but according to our data, **F** is formed on a much slower time scale in the mutant. The observed amplitude (equivalent to ~30% of the membrane dielectric) is moreover too large to account for proton movement from Glu278 to the binuclear center, which lay close to each other with respect to the membrane dielectric. We propose therefore that the origin of the fast amplitude in W164F is a vectorial proton movement from Glu278 to a pump site at or above the heme propionates and that this proton movement occurs simultaneously with the $\mathbf{A}\rightarrow\mathbf{P_R}$ transition of the catalytic cycle.

If the proton transfer that we see in the W164F mutant is associated with loading of the pump site in the $\mathbf{A}\rightarrow\mathbf{P_R}$ transition, it should also occur in the wild-type enzyme. In WT, such an event may be undetectable during normal experimental conditions due to the large electrometric response of the $\mathbf{P_R}\rightarrow\mathbf{F}$ transition. However, it could be revealed when formation of the **F** state is dramatically slowed, as in the W164F mutant. Recently, Belevich and co-workers [192] studied the generation of electric potential in WT cytochrome *c* oxidase at alkaline conditions, were the $\mathbf{P_R}\rightarrow\mathbf{F}$ and $\mathbf{F}\rightarrow\mathbf{O}$ transitions are slowed down [178]. They noticed an acceleration of the rate of the fast electrometric phase and a shortening of the initial lag, similar to our results with the W164F mutant. A comparison with optical data revealed that the fast electrometric phase develops simultaneously with the optically recorded $\mathbf{A}\rightarrow\mathbf{P_R}$ transition, which occurs when the electron at heme *a* is transferred to the binuclear center. A previous study has shown that the reaction between mixed-valence cytochrome *c* oxidase (where heme *a* and Cu_A are oxidized) and O_2 does not generate a membrane potential [137]. We can therefore conclude that the fast electric amplitude generated in the W164F mutant, as well as in wild-type at high pH, is a result of proton transfer from Glu278 to a proton acceptor above the hemes, and that this proton-transfer is kinetically linked to electron transfer into the binuclear center.

5.7 A possible mechanism for redox-linked proton transfer

A molecular mechanism of proton translocation by cytochrome *c* oxidase can be proposed based on the work presented in this thesis in combination with recent results from the Helsinki Bioenergetics group (**paper III**, **paper IV** and [113,151,192]). The model, which is schematically presented in Figure 11 relies heavily on the unique properties of water molecules enclosed in hydrophobic cavities, such as the ones located between heme *a* and the binuclear center. The proton pumping is initiated by loading of the pump site with a proton, which enables the simultaneous electron transfer from heme *a* to the active site. Full reduction of oxygen to water involves the step-wise transfer of four electrons to the binuclear center. Each of these electron transfer steps are linked to proton pumping across the membrane, which presumably occurs by the same mechanism four times during one catalytic turnover. The details of the proposed mechanism are presented below, and are for simplicity divided into different steps:

A. An electron is initially transferred from Cu_A to heme *a*. The reduction of heme *a* raises the pK_a of the pump site that is located presumably somewhere in the vicinity of heme a_3. The additional negative charge at heme *a* affects moreover the dipoles of the putative water molecules in the cavity between heme *a* and the binuclear center. The water molecules reorient themselves as a consequence of the electric field and form a hydrogen-bonded water chain that connects Glu278 with the Δ-propionate of heme a_3. The strong salt bridge between the Δ-propionate and Arg473 is weakened by the influence of the water chain and dissociates. The result is an increase in the pK_a of the propionate that attracts a proton from Glu278. The arriving proton can either stay on the propionate or alternatively be further transferred to a pump site somewhere close.

B. The additional positive charge (the proton) at or near the propionate raises the electron affinity (E_m) of heme a_3/Cu_B, after which the electron located at heme *a* is quickly transferred to the binuclear center.

C. Glu278 is reprotonated from the bulk via the D-pathway. The change in the orientation of the electric field between heme *a* and the binuclear center is sensed by the water molecules in the cavity, which reorient themselves and form a hydrogen-bonded chain that extend towards the active site. A proton can thereafter be transferred from Glu278 to the active site.

D. Glu278 is again reprotonated from the D-pathway. This proton uptake together with the neutralization of the negative charge at the binuclear center with the arrival of a substrate proton in the previous step ultimately repels electrostatically the preloaded pumped proton located at or near the heme a_3 Δ-propionate towards the P-side of the membrane.

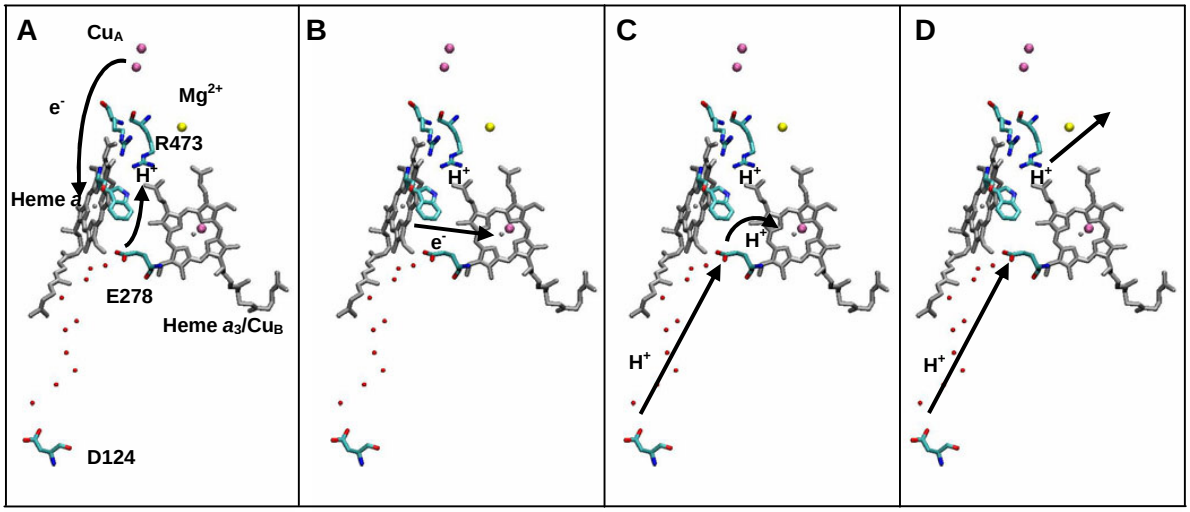

Figure 11. A schematic presentation of the proposed proton pumping mechanism. Electron transfer from heme *a* to the binuclear center is linked to proton transfer from E278, via water molecules, to a pump site located at or near the Δ-propionate of heme a_3 (A). Arg473 and the heme a_3 Δ-propionate form together a gate, which regulates the access of protons to the P-side of the membrane. When the electron reaches the catalytic site it reverses the electric field between heme *a* and heme a_3/Cu_B (B). The inverted field is sensed by the water molecules, which are located in the hydrophobic cavity close by. Rearrangement of the water dipoles then allows a proton to be transferred from Glu278 to the catalytic site (C). Upon its deprotonation, Glu278 is rapidly reprotonated via the D-pathway. The reprotonation of Glu278 after transfer of a substrate proton to the binuclear center expels the pumped proton to the P-side of the membrane (D).

5.7.1. The presented mechanism in relation to existing experimental data

In the above presented mechanism of proton transfer the pumped proton is transferred to the pump site concurrently with the transfer of an electron from heme *a* to the active site. It has been argued, that this type of mechanism cannot account for proton pumping in the $\mathbf{P_R \rightarrow F}$ transition of the catalytic cycle, since the $\mathbf{P_R \rightarrow F}$ transition is not coupled to eT to the binuclear center, which occurs already in the preceding $\mathbf{A \rightarrow P_R}$ transition. Our study of the generation of membrane potential in the W164F mutation revealed however a previously undetected electrogenic event, which became visible due to the slow formation of the ferryl state in the W164F mutant. This electrogenic event, which occurs kinetically simultaneous with the optically detected $\mathbf{A \rightarrow P_R}$ transition, was identified as loading of the pump site with a proton (**paper IV**). The corresponding phase of charge transfer goes undetectable in WT cytochrome *c* oxidase, due to the large generation of membrane potential in the subsequent $\mathbf{P_R \rightarrow F}$ transition [192]. But, in the W164F mutant, as well as in WT at high pH and in the D124N mutant, a small electrometic phase becomes visible, which corresponds to transfer of a charge about 30% of the membrane dielectric. This phase is absent in the Glu278 to glutamine mutant, and may thus represent proton transfer from Glu278 to the Δ-propionate of heme a_3 [192]. The discovery of this elementary step of the proton pumping machinery shows that a common proton pumping mechanism can be applied to all proton-transferring steps of the catalytic cycle, including the $\mathbf{P_R \rightarrow F}$ transition, since a proton is already present at the pump site at the onset of the transition.

During the reductive phase of the catalytic cycle two substrate protons are taken up to the binuclear center via the K-pathway [79,80,90]. This observation is fully compatible with our model of proton pumping. In the model, electron arrival at heme *a* results in the formation of a hydrogen-bonded water chain that connects Glu278 to the Δ-propionate of heme a_3 and allows proton transfer via a Grotthuss-type of mechanism. Next, the electron is transferred to the active site, after which the arrival of a substrate proton to the active site and the reprotonation of Glu278 expels the proton at the pump site. According to the model, all pumped protons are donated from Glu278 and the D-pathway, whereas the substrate protons can optionally be transferred via the D- or the K-pathway.

Mutation of amino acid residues in the D-pathway may create mutants, which lose their ability to translocate protons across the membrane, but sustain varying degrees of O_2 consumption activity. The D124N mutation for example severely impair catalytic activity and abolishes proton pumping [82,83]. The catalytic cycle of D124N halts at the **F**

intermediate, since proton uptake through the D-pathway from the bulk is blocked. In the recent electrometric study by Belevich and co-workers, a fast phase of membrane potential generation was observed in the D124N mutant, equivalent to the one detected at pH 10.5 for WT enzyme. The electrogenic phase was interpreted as proton transfer to the pump site located close to the Δ-propionate of heme a_3 [192]. According to this interpretation, a proton is initially transferred to the pump site also in the non-pumping D124N mutant. However, since additional protons are not available, this proton is transferred to the binuclear center and used for water formation. The lifetime of the protonated pump site in D124N is presumably very short, since experimental data indicate that the $\mathbf{P_R}\rightarrow\mathbf{F}$ transition of the D124N mutant occurs with the same rate as for WT [136]. The protonation state of the heme a_3 Δ-propionate has been shown to influence the rate of eT from heme *a* to the binuclear center [178]. A transient protonation of the Δ-propionate of heme a_3 in D124N would hence insure fast eT from heme *a* to the active site.

Another example of a mutant in the D-pathway, which has lost its ability to translocate protons across the membrane is the N131D mutant [193-195]. Quite contrary to the D124N mutation, the N131D mutation yields an enzyme with higher O_2 consumption activity than WT. The high turnover activity of the N131D mutant does not necessarily mean that the mutation has not affect the rate whereby protons are transferred through the D-pathway. Another interpretation of the observed phenomenon may be that the N131D mutation has affected the rate (increased) of a limiting step during catalytic turnover, for example by un-coupling proton translocation from the chemical reaction. It is conceivable that a proton is initially transferred to the pump site also in N131D, where after it is instantly re-routed to the active site, due to a for instance a slowed down reprotonation of Glu278. In the N131D mutant, the $\mathbf{P_R}\rightarrow\mathbf{F}$ transition shows WT transition rates, while the rate of the $\mathbf{F}\rightarrow\mathbf{O}$ transition is increased compared to WT enzyme [194]. We have shown that loading of the pump site occurs already during $\mathbf{A}\rightarrow\mathbf{P_R}$ transition, which may be why un-coupling of proton pumping from oxygen reduction does not affect the rate of $\mathbf{P_R}\rightarrow\mathbf{F}$ transition in the N131D mutant. However, if the proton pumping is abolished in the subsequent step, upon **O** formation, it can lead to an increased $\mathbf{F}\rightarrow\mathbf{O}$ transition rate, even though the rate of proton transfer via the D-pathway may be affected by the mutation.

5.7.2 Is the proton pumping mechanism common to all heme-copper oxidases?

It is appealing to think that the mechanism by which protons are pumped across the membrane would be common to all heme-copper oxidases. The thought of a general pumping mechanism is not far fetched considering that the genes encoding the heme-copper oxidases have evolved from the same ancestor. The structural homology between the mitochondrial-like cytochrome *c* oxidases and the more distantly related heme-copper oxidases, such as the ba_3 oxidase from *T. thermophilus* and the aa_3 quinol oxidase from *A. ambivalens* is however poor (discussed in chapter 5.1.1). A common pumping mechanism would consequently have to be independent from protein structure and involve other elements, such as water molecules. The importance of structurally conserved water molecules in proton transfer has recently been discussed by Sharpe and co-workers [174]. Their comparison of the existing 3D structures of heme-copper oxidases revealed that although only one amino acid residue from the D-pathway of the *R. sphaeroides* aa_3 oxidase is preserved in the *T. thermophilus* ba_3 oxidase, both oxidases contain similar water formations. An important role of water molecules in proton translocation is supported by our results in **paper I** and **II,** were we showed that different structural motifs maintain proton translocation in cytochrome *c* oxidase by providing the scaffold for formation of a hydrogen-bonded water chain through which fast proton conduction can occur.

It is not unrealistic that the mechanism of proton transfer outlined in chapter 5.7 may be generally applied to all heme-copper oxidases. The common structural feature of this super family is a low-spin heme, a high-spin heme and a copper ion located close to each other (see chapter 1.2). The near proximity of the redox centers in the heme-copper oxidases insures fast electron delivery to the binuclear center, but may also be a criterion for redox-linked proton translocation. In addition to the six histidine residues that ligate the redox centers, only three amino acid residues seem to be totally conserved in subunit I of the heme-copper oxidases [7]. Among these three residues are Arg474, which forms hydrogen bonds to both propionates of heme *a*, but not Arg473, which forms a tight ion bond with the Δ-propionate of heme a_3. Arg473 is however totally conserved amongst all other heme-copper oxidases, but the cbb_3 oxidases. The presence or absence of an arginine in the cbb_3 oxidases that corresponds to Arg473 in cytochrome *c* oxidase from *P. denitrificans* may perhaps be rethought by alternative sequence alignments. A mutational study targeted at Arg473 have indicated that proton pumping by cytochrome *c* oxidase is sustained as long as the Δ-propionate of heme a_3 receives a hydrogen bond from the surrounding protein [91]. A

recent homology model of the cbb_3 oxidase from *R. sphaeroides* implies that a lysine and a tryptophan residue are in hydrogen bonding distance of the high-spin heme [196].

A key role for water molecules in the proton pumping of the heme-copper oxidases is supported by the structure of the ba_3 oxidase from *T. thermophilus*, where one of the proposed proton pathways ends at an internal cavity close to the binuclear center [166]. The cavity contains structurally detected water molecules, which may take part in proton transfer. Whether similar structural features are present in other heme-copper oxidase remain to be seen with the appearance of x-ray structure of other non-canonical oxidases, hopefully in the near future.

6. SUMMARY

This thesis is focused on three important aspects of the redox-linked proton transfer by cytochrome *c* oxidase, namely a) the gating mechanism, whereby proton access to the different sides of the membrane is regulated, b) the role of water molecules and the conserved Glu278 in proton conduction, and c) the timing of proton transfer to the pump site, located somewhere in the vicinity of the heme a_3.

Theoretical calculations in combination with experimental data presented here pinpointed the salt bride formed by the Arg473/heme a_3 Δ-propionate pair as a possible gate that regulates proton access to the positively charged side of the membrane. Opening of the gate is determined by the redox-state between heme *a* and the binuclear center and occurs when the dipole moment of the water molecules in the cavity points towards the propionate of heme a_3. Dissociation of the Arg473/Δ-propionate pair is dependent on the hydrogen bond between the Δ-propionate and Trp164, but will not occur without the presence of water molecules in the cavity. In addition, the electrometric measurements with the W164F mutant revealed a new, undetected step in the proton pumping mechanism of cytochrome *c* oxidase, i.e. loading of the pump site, located at or near the Δ-propionate of heme a_3, in the $\mathbf{A \rightarrow P_R}$ transition of the catalytic cycle.

Glu278, an invariant amino acid among the mitochondrial-like cytochrome *c* oxidases, was shown to be dispensable for proton translocation, when other structural solutions were present that could support a long, hydrogen-bonded chain of water through which proton transfer by a Grotthuss-type of mechanism can occur.

Finally, a possible mechanism of proton transfer across the membrane was presented in which proton transfer is initiated by the protonation of the pump site and the simultaneous electron transfer between heme *a* and heme a_3. It was speculated that a common proton pumping mechanism could be applied to all heme-copper oxidases and that the mechanism could be similar to the one presented in this thesis. A common proton pumping mechanism is very likely to involve structural water molecules, since the protein structure of different heme-copper oxidases can vary substantially.

7. ACKNOWLEDGEMENTS

This study was carried out in the Helsinki Bioenergetics Group at the Institute of Biotechnology and at the Faculty of Biosciences, Division of Biochemistry, at the University of Helsinki. The work was financially supported by the Academy of Finland, the Sigrid Jusélius Foundation, the University of Helsinki, Biocentrum Helsinki, Viikki Graduate School in Biosciences, and the Magnus Ehrnrooth Foundation.

I am deeply grateful to my supervisor, Docent Anne Puustinen, for all these years. Thank you for your guidance and for sharing your knowledge of molecular biology and protein chemistry with me.

I wish to express my gratitude to Professor Mårten Wikström, the leader of Helsinki Bioenergetics Group, for providing excellent research conditions and allowing me to work in the intriguing field of bioenergetics. Your enthusiasm in cytochrome *c* oxidase and in the world of bioenergetics is inspiring and has motivated me to work hard in the laboratory.

I wish to sincerely thank Professor Michael Verkhovsky for being a patient teacher in the kinetics lab and for educative discussions on biophysics.

Professor Ilmo Hassinen and Docent Moshe Finel are acknowledged for reading the thesis manuscript and for their valuable comments and suggestions.

My warmest thanks go to all past and present members of the HBG that in any way have helped me in my work, and have provided a nice and friendly working atmosphere. I would like to especially express my appreciation to the co-authors of the articles, Marina Verkhovskaya, Mika Molin, Liisa Laakkonen, Ilya Belevich and Dmitry Bloch from HGB, and the external collaborators, Gerhard Hummer, Claudio Gomes and Miguel Teixeira.

A special thank you goes to Virve Rauhamäki, my office companion during the last years, for good discussions about science and life, and to Pamela David, a former Post Doc in HGB, for a memorable time during her years in Helsinki. The present and past technicians of HGB, Eija Haasanen, Tarja Salojärvi, Katja Sissi and Anne Hakonen, require a special mentioning due to their invaluable and excellent work. A huge thank you goes to our former secretary Satu Sankkila for her encouragement and friendship, and for always taking such good care of all the practical matters related to the laboratory.

In addition, I would like to thank all my friends and relatives, for your company on trips, during holidays and weekends and for just being there every day to cheer up my life. My sister Ann-Sofi and her family are acknowledged for their presence and support, and especially Ann-Sofi for showing what one can do with enough enthusiasm and energy.

I have dedicated my thesis to my parents, Ulla and Kurt, who have always helped and encouraged me and my sister in any way that they can. Tack för allt, mamma och pappa!

Finally, I would like to thank my husband Johnny for being such a down-to-earth, smart and supportive person that takes good care of me. Du är bäst, Johnny! And our little bundle of joy, Wilmer, so eager to learn new things and explore the world. Det är bra Wilmer att du håller mamma sysselsatt!

Helsinki, March 2007 Camilla Ribacka

8. REFERENCES

1. Brandt, U. (2006) *Annu. Rev. Biochem. 75*, 69-92.
2. Cecchini, G. (2003) *Annu. Rev. Biochem. 72*, 77-109.
3. Osyczka, A., Moser, C. C., and Dutton, P. L. (2005) *TIBS 30*, 176-182.
4. Walker, J. E. and Dickson, V. K. (2006) *Biochim. Biophys. Acta 1757*, 286-296.
5. Mitchell, P. (1961) *Nature 191*, 141-148.
6. Garcia-Horsman, J. A., Barquera, B., Rumbley, J., Ma, J., and Gennis, R. B. (1994) *J. Bacteriol. 176*, 5587-5600.
7. Pereira, M. M., Santana, M., and Teixeira, M. (2001) *Biochim. Biophys. Acta 1505*, 185-208.
8. Lübben, M. and Morand, K. (1994) *J. Biol. Chem. 269*, 21473-21479.
9. Woese, C. R. (1987) *Microbiol. Rev. 51*, 221-271.
10. Yang, D., Oyaizu, Y., Oyaizu, H., Olsen, G. J., and Woese, C. R. (1985) *Proc. Natl. Acad. Sci. USA 82*, 4443-4447.
11. John, P. and Whatley, F. R. (1977) *Biochim. Biophys. Acta 463*, 129-153.
12. van Spanning, R. J., de Boer, A. P., Reijnders, W. N., De Gier, J. W., Delorme, C. O., Stouthamer, A. H., Westerhoff, H. V., Harms, N., and van der Oost, J. (1995) *J. Bioenerg. Biomembr. 27*, 499-512.
13. Baker, S. C., Ferguson, S. J., Ludwig, B., Page, M. D., Richter, O. M., and van Spanning, R. J. (1998) *Microbiol. Mol. Biol. Rev. 62*, 1046-1078.
14. Puustinen, A., Finel, M., Virkki, M., and Wikström, M. (1989) *FEBS Lett. 249*, 163-167.
15. Richter, O. M., Tao, J., Turba, A., and Ludwig, B. (1994) *J. Biol. Chem. 269*, 23079-23086.
16. Raitio, M., Jalli, T., and Saraste, M. (1987) *EMBO J. 6*, 2825-2833.
17. De Gier, J. W., Schepper, M., Reijnders, W. N., van Dyck, S. J., Slotboom, D. J., Warne, A., Saraste, M., Krab, K., Finel, M., Stouthamer, A. H., van Spanning, R. J., and van der Oost, J. (1996) *Mol. Microbiol. 20*, 1247-1260.
18. van Verseveld, H. W., Krab, K., and Stouthamer, A. H. (1981) *Biochim. Biophys. Acta 635*, 525-534.
19. Raitio, M. and Wikström, M. (1994) *Biochim. Biophys. Acta 1186*, 100-106.
20. Wikström, M. (1977) *Nature 266*, 271-273.
21. Iwata, S., Ostermeier, C., Ludwig, B., and Michel, H. (1995) *Nature 376*, 660-669.
22. Tsukihara, T., Aoyama, H., Yamashita, E., Takashi, T., Yamaguichi, H., Shinzawa-Itoh, K., Nakashima, R., Yaono, R., and Yoshikawa, S. (1996) *Science 272*, 1136-1144.
23. Ferguson-Miller, S. and Babcock, G. T. (1996) *Chem. Rev. 7*, 2889-2907.
24. Kadenbach, B., Napiwotzki, J., Frank, V., Arnold, S., Exner, S., and Huttemann, M. (1998) *J. Bioenerg. Biomembr. 30*, 25-33.
25. Buse, G., Soulimane, T., Dewor, M., Meyer, H. E., and Bluggel, M. (1999) *Protein Science 8*, 985-990.
26. Ostermeier, C., Harrenga, A., Ermler, U., and Michel, H. (1997) *Proc. Natl. Acad. Sci. USA 94*, 10547-10553.
27. Yoshikawa, S., Shinzawa-Itoh, K., Nakashima, R., Yaono, R., Inoue, N., Yao, M., Fei, M. J., Libeu, C. P., Mizushima, T., Yamaguchi, H., Tomizaki, T., and Tsukihara, T. (1998) *Science 280*, 1723-1729.

28. Svensson-Ek, M., Abramson, J., Larsson, G., Törnroth, S., Brzezinski, P., and Iwata, S. (2002) *J. Mol. Biol. 321*, 329-339.
29. Mills, D. A., Florens, L., Hiser, C., Qian, J., and Ferguson-Miller, S. (2000) *Biochim. Biophys. Acta 1458*, 180-187.
30. Florens, L., Schmidt, B., McCracken, J., and Ferguson-Miller, S. (2001) *Biochemistry 40*, 7491-7497.
31. Lee, A., Kirichenko, A., Vygodina, T., Siletsky, S. A., Das, T. K., Rousseau, D. L., Gennis, R., and Konstantinov, A. A. (2002) *Biochemistry 41*, 8886-8898.
32. Riistama, S., Laakkonen, L., Wikström, M., Verkhovsky, M. I., and Puustinen, A. (1999) *Biochemistry 38*, 10670-10677.
33. Pfitzner, U., Kirichenko, A., Konstantinov, A. A., Mertens, M., Wittershagen, A., Kolbesen, B. O., Steffens, G. C. M., Harrenga, A., Michel, H., and Ludwig, B. (1999) *FEBS Lett. 456*, 365-369.
34. Harrenga, A. and Michel, H. (1999) *J. Biol. Chem. 274*, 33296-33299.
35. Humphrey, W., Dalke, A., and Schulten, K. (1996) *J. Mol. Graph. 14*, 33.
36. Steffens, G. C. M., Soulimane, T., Wolff, G., and Buse, G. (1993) *Eur. J. Biochem. 213*, 1149-1157.
37. Kelly, M., Lappalainen, P., Talbo, G., Haltia, T., Van der Oost, J., and Saraste, M. (1993) *J. Biol. Chem. 268*, 16781-16787.
38. Witt, H., Malatesta, F., Nicoletti, F., Brunori, M., and Ludwig, B. (1998) *Eur. J. Biochem. 251*, 367-373.
39. Riistama, S., Puustinen, A., Garcia-Horsman, A., Iwata, S., Michel, H., and Wikström, M. (1996) *Biochim. Biophys. Acta 1275*, 1-4.
40. Haltia, T., Finel, M., Harms, N., Nakari, T., Raitio, M., Wikström, M., and Saraste, M. (1989) *EMBO J. 8*, 3571-3579.
41. Echabe, I., Haltia, T., Freire, E., Goni, F. M., and Arrondo, J. L. (1995) *Biochemistry 34*, 13565-13569.
42. Bratton, M. R., Pressler, M. A., and Hosler, J. P. (1999) *Biochemistry 38*, 16236-16245.
43. Gilderson, G., Salomonsson, L., Aagaard, A., Gray, J., Brzezinski, P., and Hosler, J. (2003) *Biochemistry 42*, 7400-7409.
44. Mills, D. A., Tan, Z., Ferguson-Miller, S., and Hosler, J. (2003) *Biochemistry 42*, 7410-7417.
45. Witt, H. and Ludwig, B. (1997) *J. Biol. Chem. 272*, 5514-5517.
46. Antalis, T. M. and Palmer, G. (1982) *J. Biol. Chem. 257*, 6194-6206.
47. Zhen, Y., Hoganson, C. W., Babcock, G. T., and Ferguson-Miller, S. (1999) *J. Biol. Chem. 274*, 38032-38041.
48. Hill, B. C. (1991) *J. Biol. Chem. 266*, 2219-2226.
49. Geren, L. M., Beasley, J. R., Fine, B. R., Saunders, A. J., Hibdon, S., Pielak, G. J., Durham, B., and Millett, F. (1995) *J. Biol. Chem. 270*, 2466-2472.
50. Verkhovsky, M. I., Belevich, N., Morgan, J. E., and Wikström, M. (1999) *Biochim. Biophys. Acta 1412*, 184-189.
51. Nilsson, T. (1992) *Proc. Natl. Acad. Sci. USA 89*, 6497-6501.
52. Verkhovsky, M. I., Tuukkanen, A., Backgren, C., Puustinen, A., and Wikström, M. (2001) *Biochemistry 40*, 7077-7083.
53. Boelens, R. and Wever, R. (1979) *Biochim. Biophys. Acta 547*, 296-310.
54. Verkhovsky, M. I., Morgan, J. E., and Wikström, M. (1992) *Biochemistry 31*, 11860-11863.
55. Oliveberg, M. and Malmström, B. G. (1991) *Biochemistry 30*, 7053-7057.
56. Marcus, R. A. and Sutin, N. (1985) *Biochim. Biophys. Acta. 811*, 265-322.

57. Gray, H. B. and Winkler, J. R. (1996) *Annu. Rev. Biochem. 65*, 537-561.
58. Moser, C. C., Keske, J. M., Warncke, K., Farid, R. S., and Dutton, P. L. (1992) *Nature 355*, 796-802.
59. Page, C. C., Moser, C. C., Chen, X. X., and Dutton, P. L. (1999) *Nature 402*, 47-52.
60. Pilet, E., Jasaitis, A., Liebl, U., and Vos, M. H. (2004) *Proc. Natl. Acad. Sci. USA 101*, 16198-16203.
61. Verkhovsky, M. I., Jasaitis, A., and Wikström, M. (2001) *Biochim. Biophys. Acta 1506*, 143-146.
62. Verkhovsky, M. I., Morgan, J. E., and Wikström, M. (1995) *Biochemistry 34*, 7483-7491.
63. Agmon, N. (1995) *Chem. Phys. Lett. 244*, 456-462.
64. Cukierman, S. (2006) *Biochim. Biophys. Acta 1757*, 876-885.
65. Nagle, J. F. and Morowitz, H. J. (1978) *Proc. Natl. Acad. Sci. USA 75*, 298-302.
66. Hummer, G., Rasaiah, J. C., and Noworyta, J. P. (2001) *Nature 414*, 188-190.
67. Svensson, M., Hallen, S., Thomas, J. W., Lemieux, L., Gennis, R. B., and Nilsson, T. (1995) *Biochemistry 34*, 5252-5258.
68. Hosler, J. P., Shapleigh, J. P., Kim, Y., Pressler, M., Georgiou, C., Babcock, G. T., Alben, J. O., Ferguson-Miller, S., and Gennis, R. B. (1996) *Biochemistry 35*, 10776-10783.
69. Junemann, S., Meunier, B., Gennis, R. B., and Rich, P. (1997) *Biochemistry 36*, 14456-14464.
70. Hofacker, I. and Schulten, K. (1998) *Proteins 30*, 100-107.
71. Cukier, R. I. (2005) *Biochim. Biophys. Acta 1706*, 134-146.
72. Brändén, M., Sigurdson, H., Namslauer, A., Gennis, R. B., Ädelroth, P., and Brzezinski, P. (2001) *Proc. Natl. Acad. Sci. USA 98*, 5013-5018.
73. Kannt, A., Lancaster, C. R. D., and Michel, H. (1998) *Biophys. J. 74*, 708-721.
74. Ma, J. X., Tsatsos, P. H., Zaslavsky, D., Barquera, B., Thomas, J. W., Katsonouri, A., Puustinen, A., Wikström, M., Brzezinski, P., Alben, J. O., and Gennis, R. B. (1999) *Biochemistry 38*, 15150-15156.
75. Brändén, M., Tomson, F., Gennis, R. B., and Brzezinski, P. (2002) *Biochemistry 41*, 10794-10798.
76. Tomson, F. L., Morgan, J. E., Gu, G. P., Barquera, B., Vygodina, T. V., and Gennis, R. B. (2003) *Biochemistry 42*, 1711-1717.
77. Richter, O. M. H., Durr, K. L., Kannt, A., Ludwig, B., Scandurr, F. M., Giuffre, A., Sarti, P., and Hellwig, P. (2005) *Febs Journal 272*, 404-412.
78. Tuukkanen, A., Verkhovsky, M. I., Laakkonen, L., and Wikström, M. (2006) *Biochim. Biophys. Acta 1757*, 1117-1121.
79. Ädelroth, P., Gennis, R. B., and Brzezinski, P. (1998) *Biochemistry 37*, 2470-2476.
80. Wikström, M., Jasaitis, A., Backgren, C., Puustinen, A., and Verkhovsky, M. I. (2000) *Biochim. Biophys. Acta 1459*, 514-520.
81. Konstantinov, A. A., Siletskiy, S. A., Mitchell, D., Kaulen, A. D., and Gennis, R. B. (1997) *Proc. Natl. Acad. Sci. USA 94*, 9085-9090.
82. Thomas, J. W., Puustinen, A., Alben, J. O., Gennis, R. B., and Wikström, M. (1993) *Biochemistry 32*, 10923-10928.
83. Fetter, J. R., Qian, J., Shapleigh, J., Thomas, J. W., Garcia-Horsman, A., Schmidt, E., Hosler, J., Babcock, G. T., Gennis, R. B., and Ferguson-Miller, S. (1995) *Proc. Natl. Acad. Sci. USA 92*, 1604-1608.
84. Garcia-Horsman, J. A., Puustinen, A., Gennis, R. B., and Wikström, M. (1995) *Biochemistry 34*, 4428-4433.

85. Riistama, S., Hummer, G., Puustinen, A., Dyer, R. B., Woodruff, W. H., and Wikström, M. (1997) *FEBS Lett. 414*, 275-280.
86. Puustinen, A., Bailey, J. A., Dyer, R. B., Mecklenburg, S. L., Wikström, M., and Woodruff, W. H. (1997) *Biochemistry 36*, 13195-13200.
87. Zheng, X. H., Medvedev, D. M., Swanson, J., and Stuchebrukhov, A. A. (2003) *Biochim. Biophys. Acta 1557*, 99-107.
88. Ädelroth, P., Svensson, E. M., Mitchell, D. M., Gennis, R. B., and Brzezinski, P. (1997) *Biochemistry 36*, 13824-13829.
89. Verkhovskaya, M. L., García-Horsman, A., Puustinen, A., Rigaud, J. L., Morgan, J. E., Verkhovsky, M. I., and Wikström, M. (1997) *Proc. Natl. Acad. Sci. USA 94*, 10128-10131.
90. Belevich, I., Tuukkanen, A., Wikström, M., and Verkhovsky, M. I. (2006) *Biochemistry 45*, 4000-4006.
91. Puustinen, A. and Wikström, M. (1999) *Proc. Natl. Acad. Sci. USA 96*, 35-37.
92. Pomes, R., Hummer, G., and Wikstrom, M. (1998) *Biochim. Biophys. Acta 1365*, 255-260.
93. Tsukihara, T., Shimokata, K., Katayama, Y., Shimada, H., Muramoto, K., Aoyama, H., Mochizuki, M., Shinzawa-Itoh, K., Yamashita, E., Yao, M., Ishimura, Y., and Yoshikawa, S. (2003) *Proc. Natl. Acad. Sci. U. S. A 100*, 15304-15309.
94. Pfitzner, U., Odenwald, A., Ostermann, T., Weingard, L., Ludwig, B., and Richter, O. M. H. (1998) *J. Bioenerg. Biomembr. 30*, 89-97.
95. Lee, H. M., Das, T. K., Rousseau, D. L., Mills, D., Ferguson-Miller, S., and Gennis, R. B. (2000) *Biochemistry 39*, 2989-2996.
96. Behr, J., Michel, H., Mäntele, W., and Hellwig, P. (2000) *Biochemistry 39*, 1356-1363.
97. Popovic, D. M. and Stuchebrukhov, A. A. (2004) *FEBS Lett. 566*, 126-130.
98. Popovic, D. M. and Stuchebrukhov, A. A. (2004) *J. Am. Chem. Soc. 126*, 1858-1871.
99. Siegbahn, P. E. M., Blomberg, M. R. A., and Blomberg, M. L. (2003) *J. Phys. Chem. B 107*, 10946-10955.
100. Popovic, D. M. and Stuchebrukhov, A. A. (2005) *J. Phys. Chem. B 109*, 1999-2006.
101. Busenlehner, L. S., Salomonsson, L., Brzezinski, P., and Armstrong, R. N. (2006) *Proc. Natl. Acad. Sci. U. S. A 103*, 15398-15403.
102. Schmidt, B., McCracken, J., and Ferguson-Miller, S. (2003) *Proc. Natl. Acad. Sci USA 100*, 15539-15542.
103. Riistama, S., Puustinen, A., Verkhovsky, M. I., Morgan, J. E., and Wikström, M. (2000) *Biochemistry 39*, 6365-6372.
104. Mitchell, R. and Rich, P. R. (1994) *Biochim. Biophys. Acta 1186*, 19-26.
105. Rich, P. R. (1995) *Aust. J. Plant Physiol. 22*, 479-486.
106. Moody, A. J. (1996) *Biochim. Biophys. Acta 1276*, 6-20.
107. Moody, A. J., Cooper, C. E., and Rich, P. R. (1991) *Biochim. Biophys. Acta 1059*, 189-207.
108. Brudvig, G. W., Stevens, T. H., Morse, R. H., and Chan, S. I. (1981) *Biochemistry 20*, 3912-3921.
109. Baker, G. M., Noguchi, M., and Palmer, G. (1987) *J. Biol. Chem. 262*, 595-604.
110. Morgan, J. E., Blair, D. F., and Chan, S. I. (1985) *J. Inorg. Biochem. 23*, 295-302.
111. Antalik, M., Jancura, D., Palmer, G., and Fabian, M. (2005) *Biochemistry 44*, 14881-14889.
112. Verkhovsky, M. I., Jasaitis, A., Verkhovskaya, M. L., Morgan, L., and Wikström, M. (1999) *Nature 400*, 480-483.

113. Bloch, D., Belevich, I., Jasaitis, A., Ribacka, C., Puustinen, A., Verkhovsky, M. I., and Wikström, M. (2004) *Proc. Natl. Acad. Sci. USA 101*, 529-533.
114. Wikström, M. (2004) *Biochim. Biophys. Acta 1655*, 241-247.
115. Ruitenberg, M., Kannt, A., Bamberg, E., Fendler, K., and Michel, H. (2002) *Nature 417*, 99-102.
116. Chance, B., Saronio, C., and Leigh, J. S., Jr. (1975) *J. Biol. Chem. 250*, 9226-9237.
117. Verkhovsky, M. I., Morgan, J. E., and Wikström, M. (1994) *Biochemistry 33*, 3079-3086.
118. Wikström, M. (1981) *Proc. Natl. Acad. Sci. USA 78*, 4051-4054.
119. Babcock, G. T. and Wikström, M. (1992) *Nature 356*, 301-309.
120. Proshlyakov, D. A., Ogura, T., Shinzawa-Itoh, K., Yoshikawa, S., Appelman, E. H., and Kitagawa, T. (1994) *J. Biol. Chem. 269*, 29385-29388.
121. Proshlyakov, D. A., Ogura, T., Shinzawa-Itoh, K., Yoshikawa, S., and Kitagawa, T. (1996) *Biochemistry 35*, 76-82.
122. Proshlyakov, D. A., Pressler, M. A., and Babcock, G. T. (1998) *Proc. Natl. Acad. Sci. USA 95*, 8020-8025.
123. Fabian, M., Wong, W. W., Gennis, R. B., and Palmer, G. (1999) *Proc. Natl. Acad. Sci USA 96*, 13114-13117.
124. Hallen, S. and Nilsson, T. (1992) *Biochemistry 31*, 11853-11859.
125. Mitchell, R., Mitchell, P., and Rich, P. R. (1992) *Biochim. Biophys. Acta 1101*, 188-191.
126. Oliveberg, M., Hallén, S., and Nilsson, T. (1991) *Biochemistry 30*, 436-440.
127. Karpefors, M., Ädelroth, P., Namslauer, A., Zhen, Y. J., and Brzezinski, P. (2000) *Biochemistry 39*, 14664-14669.
128. Morgan, J. E., Verkhovsky, M. I., and Wikström, M. (1996) *Biochemistry 35*, 12235-12240.
129. Morgan, J. E., Verkhovsky, M. I., Palmer, G., and Wikström, M. (2001) *Biochemistry 40*, 6882-6892.
130. Proshlyakov, D. A., Pressler, M. A., DeMaso, C., Leykam, J. F., Dewitt, D. L., and Babcock, G. T. (2000) *Science 290*, 1588-1591.
131. Iwaki, M., Breton, J., and Rich, P. R. (2002) *Biochim. Biophys. Acta 1555*, 116-121.
132. Iwaki, M., Puustinen, A., Wikström, M., and Rich, P. R. (2003) *Biochemistry 42*, 8809-8817.
133. Sucheta, A., Szundi, I., and Einarsdottir, O. (1998) *Biochemistry 37*, 17905-17914.
134. Iwaki, M., Puustinen, A., Wikström, M., and Rich, P. R. (2006) *Biochemistry 45*, 10873-10885.
135. Karpefors, M., Ädelroth, P., Zhen, Y. J., Ferguson-Miller, S., and Brzezinski, P. (1998) *Proc. Natl. Acad. Sci. USA 95*, 13606-13611.
136. Smirnova, I., Ädelroth, P., Gennis, R. B., and Brzezinski, P. (1999) *Biochemistry 38*, 6826-6833.
137. Jasaitis, A., Verkhovsky, M. I., Morgan, J. E., Verkhovskaya, M. L., and Wikström, M. (1999) *Biochemistry 38*, 2697-2706.
138. Faxen, K., Gilderson, G., Ädelroth, P., and Brzezinski, P. (2005) *Nature 437*, 286-289.
139. Verkhovsky, M. I., Morgan, J. E., and Wikström, M. (1996) *Proc. Natl. Acad. Sci. USA 93*, 12235-12239.
140. Zaslavsky, D., Sadoski, R. C., Wang, K., Durham, B., Gennis, R. B., and Millett, F. (1998) *Biochemistry 37*, 14910-14916.
141. Wikström, M. (1998) *Biochim. Biophys. Acta 1365*, 185-192.
142. Brzezinski, P. and Larsson, G. (2003) *Biochim. Biophys. Acta 1605*, 1-13.

143. Krab, K. and Wikström, M. (1987) *Biochim. Biophys. Acta 895*, 25-39.
144. Morgan, J. E., Verkhovsky, M. I., and Wikström, M. (1994) *J. Bioenerg. Biomembr. 26*, 599-608.
145. Malmström, B. G. (1989) *FEBS Lett. 250*, 9-21.
146. Wikström, M. (1989) *Nature 338*, 776-778.
147. Wikström, M. and Morgan, J. E. (1992) *J. Biol. Chem. 267*, 10266-10273.
148. Verkhovsky, M. I., Morgan, J. E., Verkhovskaya, M., and Wikström, M. (1997) *Biochim. Biophys. Acta 1318*, 6-10.
149. Michel, H. (1999) *Biochemistry 38*, 15129-15140.
150. Papa, S., Capitanio, N., Capitanio, G., and Palese, L. L. (2004) *Biochim. Biophys. Acta 1658*, 95-105.
151. Wikström, M., Verkhovsky, M. I., and Hummer, G. (2003) *Biochim. Biophys. Acta 1604*, 61-65.
152. Raitio, M., Pispa, J. M., Metso, T., and Saraste, M. (1990) *FEBS Lett. 261*, 431-435.
153. Kovach, M. E., Phillips, R. W., Elzer, P. H., Roop, R. M., and Peterson, K. M. (1994) *Biotechniques 16*, 800-802.
154. Mitchell, P., Moyle, J., and Mitchell, R. (1979) *Methods Enzymol. 55*, 627-640.
155. Wikström, M. and Penttilä (1982) *FEBS Lett. 144*.
156. Rigaud, J. L., Pitard, B., and Levy, D. (1995) *Biochim. Biophys. Acta 1231*, 223-246.
157. Gibson, Q. H. and Greenwood, C. (1963) *Biochem. J. 86*, 541-554.
158. Drachev, L. A., Jasaitis, A. A., Kaulen, A. D., Kondrashin, A. A., Liberman, E. A., Nemecek, I. B., Ostroumov, S. A., Semenov, A. Y., and Skulachev, V. P. (1974) *Nature 249*, 321-324.
159. Cornell, W. D., Cieplak, P., Bayly, C. I., Gould, I. R., Merz, K. M., Ferguson, D. M., Spellmeyer, D. C., Fox, T., Caldwell, J. W., and Kollman, P. A. (1995) *J. Am. Chem. Soc. 117*, 5179-5197.
160. Pearlman, D. A., Case, D. A., Caldwell, J. W., Ross, W. S., Cheatham, T. E., Debolt, S., Ferguson, D., Seibel, G., and Kollman, P. (1995) *Computer Physics Communications 91*, 1-41.
161. Thomas, J. W., Calhoun, M. W., Lemieux, L. J., Puustinen, A., Wikström, M., Alben, J. O., and Gennis, R. B. (1994) *Biochemistry 33*, 13013-13021.
162. Pereira, M. M., Verkhovskaya, M. L., Teixeira, M., and Verkhovsky, M. I. (2000) *Biochemistry 39*, 6336-6340.
163. Kannt, A., Soulimane, T., Buse, G., Becker, A., Bamberg, E., and Michel, H. (1998) *FEBS Lett. 434*, 17-22.
164. Honnami, K. and Oshima, T. (1984) *Biochemistry 23*, 454-460.
165. Pereira, M. M., Santana, M., Soares, C. M., Mendes, J., Carita, J. N., Fernandes, A. S., Saraste, M., Carrondo, M. A., and Teixeira, M. (1999) *Biochim. Biophys. Acta 1413*, 1-13.
166. Soulimane, T., Buse, G., Bourenkov, G. P., Bartunik, H. D., Huber, R., and Than, M. E. (2000) *EMBO Journal 19*, 1766-1776.
167. Keightley, J. A., Zimmermann, B. H., Mather, M. W., Springer, P., Pastuszyn, A., Lawrence, D. M., and Fee, J. A. (1995) *J. Biol. Chem. 270*, 20345-20358.
168. Das, T. K., Gomes, C. M., Teixeira, M., and Rousseau, D. L. (1999) *Proc. Natl. Acad. Sci. USA 96*, 9591-9596.
169. Purschke, G. W., Schmidt, C. L., Petrsen, A., and Schafer, G. (1997) *J. Bacteriol. 179*, 1344-1353.
170. Aagaard, A., Gilderson, G., Mills, D. A., Ferguson-Miller, S., and Brzezinski, P. (2000) *Biochemistry 39*, 15847-15850.

171. Salomonsson, L., Lee, A., Gennis, R. B., and Brzezinski, P. (2004) *Proc. Natl. Acad. Sci. USA 101*, 11617-11621.
172. Olkhova, E., Hutter, M. C., Lill, M. A., Helms, V., and Michel, H. (2004) *Biophys. J. 86*, 1873-1889.
173. Cukier, R. I. (2004) *Biochim. Biophys. Acta 1656*, 189-202.
174. Sharpe, M. A., Qin, L., and Ferguson-Miller, S. (2005) in *Biophysical and Structural Aspects of Bioenergetics* (Mårten Wikström, Ed.) pp 26-54, RSC Publishing, Cambridge, UK.
175. Warshel, A. (1981) *Biochemistry 20*, 3167-3177.
176. Pereira, M. M., Sousa, F. L., Teixeira, M., Nyquist, R. M., and Heberle, J. (2006) *FEBS Letters 580*, 1350-1354.
177. Behr, J., Hellwig, P., Mäntele, W., and Michel, H. (1998) *Biochemistry 37*, 7400-7406.
178. Brändén, G., Brändén, M., Schmidt, B., Mills, D. A., Ferguson-Miller, S., and Brzezinski, P. (2005) *Biochemistry 44*, 10466-10474.
179. Lee, Y. S. and Krauss, M. (2004) *J. Am. Chem. Soc. 126*, 2225-2230.
180. Seibold, S. A., Mills, D. A., Ferguson-Miller, S., and Cukier, R. I. (2005) *Biochemistry 44*, 10475-10485.
181. Mills, D. A., Geren, L., Hiser, C., Schmidt, B., Durham, B., Millett, F., and Ferguson-Miller, S. (2005) *Biochemistry 44*, 10457-10465.
182. Kornblatt, J. A., Kornblatt, M. J., Rajotte, I., Gaston, H. B. H., and Kahn, P. C. (1998) *Biophys. J. 75*, 435-444.
183. Mills, D. A. and Ferguson-Miller, S. (2002) *Biochim. Biophys. Acta 1555*, 96-100.
184. Junemann, S., Heathcote, P., and Rich, P. R. (2000) *Biochim. Biophys. Acta 1456*, 56-66.
185. Pecoraro, C., Gennis, R. B., Vygodina, T. V., and Konstantinov, A. A. (2001) *Biochemistry 40*, 9695-9708.
186. Watmough, N. J., Cheesman, M. R., Greenwood, C., and Thomson, A. J. (1994) *Biochem. J. 300*, 469-475.
187. Brittain, T., Little, R. H., Greenwood, C., and Watmough, N. J. (1996) *FEBS Lett. 399*, 21-25.
188. Moody, A. J. and Rich, P. R. (1994) *Eur. J. Biochem. 226*, 731-737.
189. Vygodina, T. and Konstantinov, A. (1989) *Biochim. Biophys. Acta 973*, 390-398.
190. Fabian, M. and Palmer, G. (2001) *Biochemistry 40*, 1867-1874.
191. Hill, B. C. and Greenwood, C. (1984) *Biochem. J. 218*, 913-921.
192. Belevich, I., Verkhovsky, M. I., and Wikström, M. (2006) *Nature 440*, 829-832.
193. Pfitzner, U., Hoffmeier, K., Harrenga, A., Kannt, A., Michel, H., Bamberg, E., Richter, O. M., and Ludwig, B. (2000) *Biochemistry 39*, 6756-6762.
194. Pawate, A. S., Morgan, J., Namslauer, A., Mills, D., Brzezinski, P., Ferguson, M., and Gennis, R. B. (2002) *Biochemistry 41*, 13417-13423.
195. Namslauer, A., Pawate, A. S., Gennis, R., and Brzezinski, P. (2003) *Proc. Natl. Acad. Sci. USA 100*, 15543-15547.
196. Sharma, V., Puustinen, A., Wikström, M., and Laakkonen, L. (2006) *Biochemistry 45*, 5754-5765.